공학박사학위논문

Effect of Post-Annealing on the Microstructure and Properties of Low Temperature Chemical-Vapor-Deposited Carbides (TaC, HfC, SiC)

후열처리가 저온 화학기상증착법으로 증착한 탄화물 (TaC, HfC, SiC)의 미세구조와 특성에 미치는 영향

2023년 8월

서울대학교 대학원

재료공학부

한 장 원

Effect of Post-Annealing on the Microstructure and Properties of Low Temperature Chemical-Vapor-Deposited Carbides (TaC, HfC, SiC)

지도 교수 박 찬

이 논문을 공학박사 학위논문으로 제출함

2023 년 7 월

서울대학교 대학원

재료공학부

한 장 원

한장원의 공학박사 학위논문을 인준함

2023 년 7 월

위 원 장 유 상 임 (인)

부위원장 박 찬 (인)

위 원 정 인 호 (인)

위 원 박 지 연 (인)

위 원 한 인 섭 (인)

Abstract

Effect of Post-Annealing on the Microstructure and Properties of Low temperature Chemical-Vapor-Deposited Carbides (TaC, HfC, SiC)

Jangwon Han

Department of Materials Science & Engineering

Graduate school

Seoul National University

To investigate the effect of post-annealing on the microstructure and properties of low temperature chemical-vapor-deposited carbides (TaC, HfC, SiC), carbide films were deposited on graphite substrates by CVD and post-annealed at different conditions, and the relation between the deposition/post-annealing conditions and the microstructure/mechanical properties were studied.

Tantalum carbide (TaC) coating layers were deposited on graphite substrates using

the $TaCl_5$-C_3H_6-H_2 CVD system under various deposition conditions. The deposited TaC coating layers exhibited crystallographic preferred orientation, with (111) and (200) orientations being dominant. As the deposition temperature was increased, the preferred orientation changed to random orientations. Subsequent post-annealing significantly improved the crystallinity of the coating layers. When deposited at 1100°C to 1300°C, the microstructure exhibited columnar structures and columnar-equiaxed mixed structures. However, subsequent post-annealing resulted in grain growth, causing the transformation of the microstructure from columnar to equiaxed form. These findings highlight the ability of post-annealing to enhance crystallinity and induce mechanical property changes of up to 10% increase in TaC coating layers.

Hafnium carbide (HfC) coating layers were deposited on graphite substrates using the $HfCl_4$–C_3H_6–H_2 CVD system at 1200°C. The as-deposited coating layers exhibited high crystallinity and dense microstructures (columnar-like structure). Post-annealing further affected the microstructures, transforming columnar structures into equiaxed structures and causing the coalescence of pores. The nano hardness of the coating layer was also improved during the post-annealing process. These results demonstrate that HfC coating layers deposited at 1200°C possess dense microstructures, and their crystallinity and nano hardness can be enhanced through post-annealing.

Silicon carbide (SiC) coating layers were deposited on graphite substrates using the CVD method at various deposition temperatures. X-ray diffraction (XRD) analyses revealed changes in crystallinity depending on the deposition temperature. When

layers were deposited at 900°Cs, peaks of free silicon (Si) were observed, while they were absent at layers deposited at high temperatures due to the complete reaction of the precursor. The microstructure showed a tendency for increased thickness at higher deposition temperatures. Post-annealing improved the crystallinity of the deposited coating layers. The nano hardness of the coating layers also exhibited temperature-dependent variations. These findings suggest that post-annealing can modify the crystallinity, microstructure, and nano hardness of SiC coating layers.

Furthermore, although TaC, HfC, and SiC are carbide-based coating layers, their growth mechanisms of the microstructure are slightly different. Therefore, the changes in the microstructure during the post-annealing process vary. In particular, TaC, HfC, and SiC exhibited partial differences after the post-annealing process, which were briefly discussed.

This study provides comprehensive and detailed insights into the properties of high-temperature ceramic carbides (TaC, HfC, SiC) through the investigation of their crystallinity, microstructure, and the effects of post-annealing on the microstructure/mechanical properties. The findings contribute to a better understanding of the superior properties exhibited by these high-temperature ceramic carbides.

Key words: Chemical vapor deposition, Low temperature, Tantalum carbide, Hafnium carbide, Silicon carbide, Post-annealing, nano-indentation,

Crystallinity

Student number: 2015-30186

Table of Contents

List of Figures

List of Tables

Chapter 1. General introduction

1. Introduction

Refractory transition metal borides, nitrides, and carbides are known as ultra-high-temperature ceramics (UHTCs) due to their extremely high melting points exceeding 3000°C[1-5]. In the early era of high-temperature ceramics, UHTC material selection was based on melting temperature, but the oxidation temperature and melting points of oxides are actually more crucial[1-2]. However, limited manufacturing techniques have posed challenges in material development.[4-5] These materials have garnered interest as potential candidates for applications such as thermal protection systems (TPS) for hypersonic vehicles [6-7], turbine blades [4, 6], gas nozzles [4], and ceramic susceptors [8-9]. Among refractory transition metal borides, nitrides, and carbides, research on carbide materials is still challenging [4.].

Depending on the bonding mechanism of carbide materials, they can be classified into interstitial carbides and covalent carbides[10]. The melting point of the material can be considered as influenced by the bonding mechanism. Most interstitial carbides have melting points above 3000°C, while covalent carbides have melting points lower than 3000°C. Tantalum carbide (3983°C) and Hafnium carbide (3930°C) are classified as interstitial carbides, while Silicon carbide (2730°C) can be classified as a covalent carbide[10-11]. Due to their high melting points, they can achieve high density when manufactured using sintering methods. However, when manufactured using the chemical vapor deposition (CVD) method, it is possible to produce them

at lower temperatures compared to sintering. Despite some similarities in CVD microstructure growth mechanisms due to their high melting points, ultimately, differences are observed in microstructure and properties.

Carbides produced by CVD are known to exhibit high crystallinity and mechanical properties when manufactured at high temperatures, particularly around 1400°C. However, when produced at high temperatures, issues such as pore structures existing within the microstructure and damage of fiber in the process of manufacturing fiber-reinforced composites can arise.

Despite exhibiting excellent mechanical properties and oxidation resistance at high temperatures, carbides such as TaC and HfC, which are interstitial carbides, consistently face issues such as microstructural problems occurring during high-temperature manufacturing and thermal stability problems after usage, resulting in coating layer detachment or fracture. Additionally, manufacturing a dense coating layer with a sufficient thickness at low temperatures remains a challenging issue.

In the case of TaC, various methods, including Filament CVD, have been applied to achieve low temperature manufacturing [13-14]. However, the presence of secondary phases, including Ta_2C, within the microstructure has been identified as a cause of decreased mechanical properties[13-14]. Therefore, it is necessary to control the secondary phases while depositing at low temperatures to ensure both the deposition of the coating layer and the desired mechanical properties[15]. In this dissertation, TaC coating layers were deposited at relatively low temperatures, and their microstructure was controlled through post-annealing processes to achieve similar

values of crystallinity and mechanical properties as those obtained from high-temperature manufacturing.

In contrast to TaC, depositing HfC at relatively low temperatures poses a significantly tricky challenge in obtaining a dense microstructure. Changing the precursor of carbon to lower the temperature is an option; however, this introduces issues such as the presence of carbon soot within the microstructure and a decrease in crystallinity. Thus, research is needed to address these problems and manufacture HfC coating layers. In this dissertation, dense microstructures were deposited at low temperatures, and their mechanical properties were improved through post-annealing processes.

SiC, a covalent carbide, has been extensively studied and applied, even in fiber-reinforced composite forms[18-20]. However, delamination issues after usage at high temperatures are still observed[19-20]. In this dissertation, the changes in crystallinity due to post-annealing of SiC coating layers deposited at low temperatures and their correlation with microstructure were investigated.

While TaC and HfC are interstitial carbides and SiC is a covalent carbide, all belonging to the same carbide category, they exhibit differences in the deposition mechanisms of coating layers. Therefore, slight differences in microstructural changes can be observed between the initial manufacturing process and subsequent post-annealing. In particular, interstitial carbides follow models such as Van der Drift[21] and Structural Zone Modeling (SZM) for their growth [12], whereas SiC has a unique microstructure growth model[22]. The microstructures of interstitial carbides

manufactured through conventional high-temperature processes were prone to delamination due to adhering to models like Van der Drift. Hence, it is crucial to control such microstructures to maintain integrity even at high temperatures. To address these issues, manufacturing dense microstructures at low temperatures and inducing equiaxed microstructure changes through post-annealing via epitaxial growth is recommended

In this dissertation, to establish the correlation of characteristics of crystallinity, microstructure, and relative orientation of carbide coating layers, ceramic carbide (TaC, HfC, SiC) coating layers were deposited on a graphite substrate at temperatures similar to or relatively lower than previous ones by modifying the deposition parameters, and their characteristics were analyzed (Chapter 5). Post-annealing was performed for observing changes in the crystallinity and microstructure of the deposited coating, followed by characterization (Chapter 6). The influence of the changed crystallinity and microstructure of the deposited coating layer through the effect of post-annealing on the nano hardness was investigated (Chapter 7).

Rest of the thesis is organized into the following chapters:

Chapter 2: Background knowledge pertinent to this dissertation is presented.

Chapter 3: Reviews of previously reported literatures related with this study are introduced.

Chapter 4: Experimental techniques and characterization method used in this

dissertation are introduced.

Chapter 5: High temperature ceramic carbides (TaC, HfC, SiC) deposited using chemical vapor deposition are presented.

Chapter 6: Effects of post-annealing on property enhancement of high temperature ceramic carbide (TaC, HfC, SiC) coating layers are presented.

Chapter 7: Changes in mechanical properties of ceramic carbides during post-annealing are presented.

Chapter 8: A brief summary of the present work is provided.

1.2 Aim and objective

The processing temperature for carbides (TaC, HfC, SiC) manufactured by CVD is typically above 1300°C. However, when manufactured at high temperatures, issues such as microstructure and thermal stability may arise. Therefore, in this study, we aimed to improve the properties of TaC, HfC, and SiC materials by depositing them at relatively low temperatures using the CVD method on graphite substrates, followed by a post-annealing process.

ⅰ) We deposited carbide (TaC, HfC, SiC) ceramics at relatively low temperatures on a graphite substrate using the chemical vapor deposition method.

ⅱ) We applied a post-annealing process to the deposited coating layers to improve properties such as microstructure, crystallinity, and nano hardness.

To study the effect of the post-annealing process on the crystallinity, microstructure, and mechanical properties of high-temperature carbide ceramics fabricated by a low-temperature CVD process. Additionally, we explained the microstructural growth behavior of TaC and HfC, which had not been previously presented, using the growth mechanism of the Drift model and provided a morphological map. Ultimately, we induced property improvement through post-annealing.

1.3 References

1. M. M. Opeka, I. G. Talmy, J. A. Zaykoski, *Oxidation-based materials selection for 2000◦C + hypersonic aerosurfaces: Theoretical considerations and historical experience*, J. Mater. Sci., 39 (2004) 5887–5904

2. A. Paul, S. Venugopal, J.G.P. Binner, B. Vaidhyanathan, A.C.J. Heaton, P.M. Brown, *UHTC–carbon fibre composites: Preparation, oxyacetylene torch testing and characterization*, J. Eur. Ceram. Soc., 33 (2013) 423–432

3. William G. Fahrenholtz, Greg E. Hilmas, *Ultra-high temperature ceramics: Materials for extreme environments*, Scripta Mater., 129 (2017) 94–99

4. E. Wuchina, E. Opila, M. Opeka, W. Fahrenholtz, I. Talmy, *UHTCs: Ultra-High Temperature Ceramic Materials for Extreme Environment Applications*, Electrochem. Soc. Interface, 16(4) (2007)

5. A. Sayir, *Carbon fiber reinforced hafnium carbide composite*, J. Mater. Sci., 39 (2004) 5995–6003

6. S. Tang, C. Hu, Design, *Preparation and Properties of Carbon Fiber Reinforced Ultra-High Temperature Ceramic Composites for Aerospace Applications: A Review*, J. Mater. Sci. Technol., 33 (2017) 117–130

7. N. P. Padture, *Advanced structural ceramics in aerospace propulsion*, Nat. Mater., 15(8) (2016) 804–809

8. I. T. Martin, C. W. Teplin, P. Stradins, M. Landry, M. Shub, R. C. Reedy, Bobby To, J. V. Portugal, J. T. Mariner, *High rate hot-wire chemical vapor deposition of silicon thin films using a stable TaC covered graphite filament*, Thin Solid Films, 519 (2011) 4585–4588

9. D. Nakamura, T. Kimura, T. Narita, A. Suzumura, T. Kimoto, K. Nakashima, *TaC-coated graphite prepared via a wet ceramic process: Application to CVD susceptors for epitaxial growth of wide-bandgap semiconductors*, J. Cryst. Growth, 478 (2017) 163–173

10. H. O. Pierson, *Handbook of Chemical Vapor Deposition (CVD) Principles, Technology, and Applications*, NOYES PUBLICATIONS (1999)

11. G.B. Thompson, C.R. Weinberger, *Ultra-High Temperature Ceramics: Materials for Extreme Environment Applications*, John Wiley & Sons (2014)

12. M. Ohring, *Materials Science of Thin films*, Academic Press (2002)

13. M. Ali, M. Ürgen, M.A. Atta, *Tantalum carbide films synthesized by hot-filament chemical vapor deposition technique*, Surf. Coat. Tech., 206 (2012) 2833–2838

14. F. Togashi, K. Kobayashi, M. Mitsuhashi, S. Karasawa, S. Ohya, T. Watanabe, *Synthesis and morphology of CVD diamond on Ta and TaC film*, J. Cryst. Growth, 128 (1993) 418-424

15. Z.-K. Chen, X. Xiong, Y. Long, *Influence of $TaCl_5$ partial pressure on texture structure of TaC coating deposited by chemical vapor deposition*, Appl. Surf. Sci.,

257 (2011) 4044–4050

16. Y.-L. Wang, X. Xiong, G.-D. Li, H.-B. Zhang, Z.-K. Chen, W. Sun, X.-J. Zhao, *Microstructure and ablation behavior of hafnium carbide coating for carbon/carbon composites*, Surf. Coat. Tech. 206 (2012) 2825–2832

17. Y.-L. Wang, X. Xiong, X.-J. Zhao, G.-D. Li, Z.-K. Chen, W. Sun, *Structural evolution and ablation mechanism of a hafnium carbide coating on a C/C composite in an oxyacetylene torch environment*, Corros. Sci., 61 (2012) 156–161

18. H. Dong, X. Gao, S. Zhang, Y. Song, J. Yang, Fang Wang, *Effects of heat treatment on the mechanical properties at elevated temperatures of plain-woven SiC/SiC composites*, J. Eur. Ceram. Soc., 42 (2022) 412–419

19. X. Han, X. Chen, J. Ding, W. Wu, Z. Sun, Y. Song, *Influence of heat treatment on microstructure and mechanical properties of Cansas-II SiC/PyC/CVI-SiC mini-composites*, Ceram. Int., 48 (2022) 1077–1089

20. H. Mei, H. Zhang, W. Huang, M. Han, Y. Xu, L. Cheng, *Effects of heat treatment temperatures on microstructures and mechanical properties of the chopped carbon fibres SiC composites*, Adv. Appl. Ceram., 117 [7] (2018) 389–394

21. F. Silva, F. Be´ne´dic, P. Bruno, A. Gicquel, *Formation of <110> texture during nanocrystalline diamond growth: an X-ray diffraction study*, Diam. Relat. Mater., 14 (2005) 398–403

22. J. Chin, P. K. Gantzel, R. G. Hudson, *The Structure of Chemical Vapor Deposited*

Silicon Carbide, Thin Solid Films 40 (1977) 57–72

Chapter 2. General backgrounds

2.1. High temperature ceramics and applications

High temperature ceramic materials are materials with high melting points, primarily composed of refractory metals from groups Ⅳ-Ⅴ of the periodic table, as shown in Figure 2-1, combined with elements such as C, B, and N.[1-6] Ceramics combined with refractory metals can be classified as interstitial carbides and covalent carbides combined with B and Si.[7-8] These materials exhibit characteristics such as high chemical stability, mechanical properties, and oxidation resistance in high temperature environments.

The history of high temperature ceramics is shown in Figure 2-2. High temperature ceramic materials were discovered in the late 1800s, but their practical use began in the 1960s. During this time, limited fabricating technologies and materials led to the predominant use of Si-based substances such as SiC and Si_3N_4. Subsequently, with advancements in fabricating technology and expanded material selection, various materials started to be utilized, and the demand increased from high temperature aerospace applications to the energy sector. Until the 2010s, the emphasis was primarily on fabricating techniques. However, since then, the focus has shifted towards developing improved ceramic materials, considering factors such as material quality, changes in properties based on chemical stoichiometry, variations in fabricating temperature, increased oxidation resistance, and fabricating based on

design forms.

High temperature ceramic materials are primarily used in fields where excellent properties in terms of nuclear, high-temperature, chemical, and mechanical characteristics are required. Due to their outstanding high temperature performance and durability, they are utilized in a wide range of temperatures, starting from low temperatures around 300°C to high temperatures exceeding 2000°C.

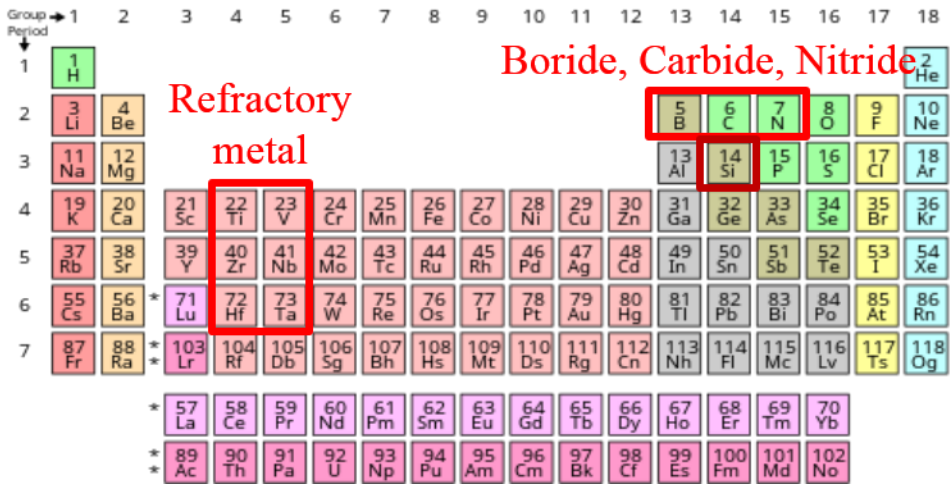

Figure 2-1. The main materials for high-temperature ceramics include refractory transition metals along with B, C, and N.

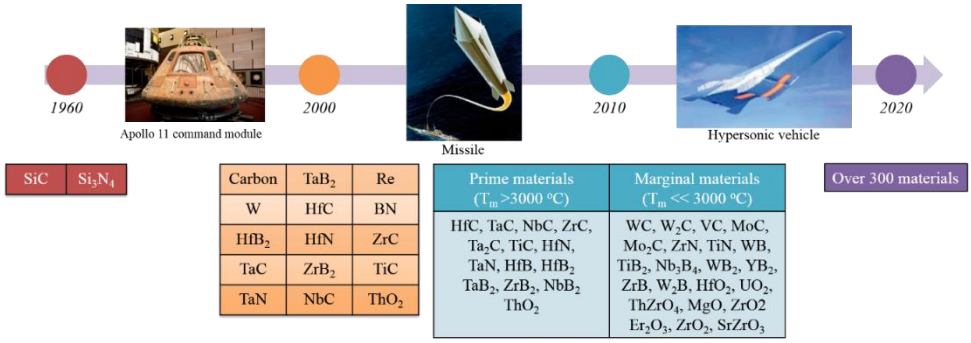

Figure 2-2. Development history of high temperature ceramics.

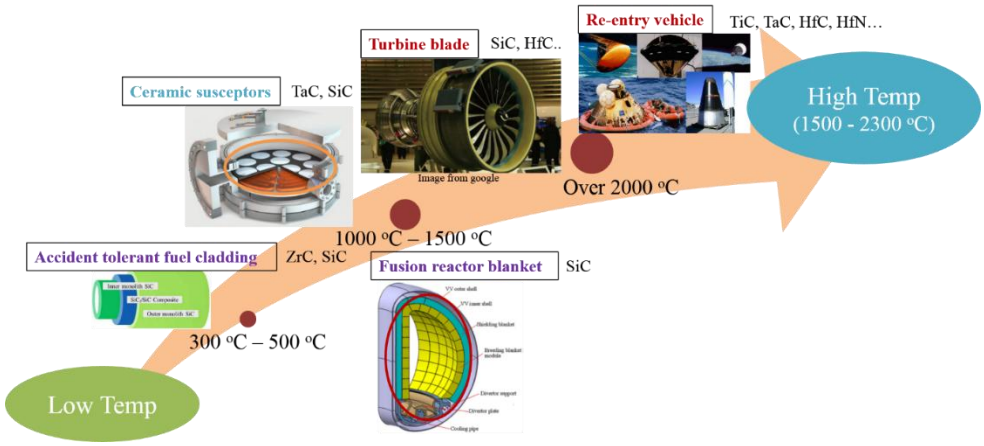

Figure 2-3. High temperature ceramic materials find applications in extreme environments, ranging from low temperature to high temperature regions.

2.2 High temperature carbide ceramics

Refractory transition metal carbides (ZrC, HfC, TaC, NbC, etc.) show good performance (thermal/mechanical properties) in ultra-high temperature regions. They are commonly manufactured in the form of compacts and widely used in tools requiring high wear resistance[7-8]. TaC, HfC, SiC, and other carbides are utilized in compact form, coating layers, and composite structures. They are particularly prevalent in fields that demand high-temperature oxidation resistance, such as aerospace applications.

Chemical vapor deposition (CVD) processes are widely used to produce materials in their finished form, which cannot be easily manufactured through conventional methods. Most elements can be deposited by either electroplating or physical vapor deposition (including sputtering, ion plating, and vacuum deposition)[9]. However, the latter process cannot deposit high-melting-point elements such as tungsten, tantalum, or carbon. Electroplating techniques cannot be used to deposit specific elements of commercial importance, such as molybdenum, tungsten, and silicon. CVD processes offer the additional advantage of being able to deposit compounds, including oxides, nitrides, and carbides, as well as many alloys.

During the deposition process for thin films using the CVD method, films acquire orientation. At this point, the growth mechanism of the deposited thin films can be classified into two different theories: one based on the growth process and the other based on the driving forces.

Distinguished by the growth process, it can be divided into two stages: the initial stage and the later stage, as proposed by Bauer for the initial stage[11-12]. The thin film growth mechanism at this stage is primarily influenced by the driving force of surface energy and substrate effects. Four main considerations are essential. Firstly, the adatom-adatom energy should exceed the adatom-substrate energy. Secondly, a low nucleation rate is crucial. Additionally, maintaining a super-saturation unaffected by substrate defects is important. Finally, the presence of well-grown nuclei displaying a crystallographic phase is significant[11-12]. Furthermore, to minimize the substrate's influence, an amorphous substrate is considered most suitable.

In the later stage, the growth mechanism is mostly explained by Drift (Figure 2-4), following an evolutionary selection process[13-15]. This means that the growth direction is determined by the stress applied to the film during the growth process or favoring growth in the direction of higher thermal conductivity. Consequently, at low temperatures, growth occurs predominantly in the vertical direction, while increasing the deposition temperature leads to horizontal growth[14]. The initial growth process under Drift exhibits a microstructure similar to the columnar structure discussed in the vapor deposition mechanism's structural zone modeling.

Normally, the deposition of thin films shows typical thermodynamic growth involving nuclei gathering to grow in a spherical form, although it may vary depending on the shape of the nuclei. The theory proposed by Walton-Rhodin is based on an atomistic theory where nuclei form clusters[16-17]. Unlike the preceding

growth process, the growth mechanism is influenced by the shape of the nuclei and surface energy. Thus, nuclei with different shapes such as line, L-shaped, triangular, or square can cluster together and grow[16]. In cases where the growth is influenced by surface energy, which is based on Pelleg's theory[18-19], it is known that the driving force for growth is determined by the atom (or vapor) concentration. To control the growth of thin films, it is affected by reducing surface energy and the density of ledges formed by atom concentration.

Coating layers deposited using the CVD method typically exhibit a columnar growth microstructure[10]. However, carbides show slightly different microstructural growth tendencies. While carbides generally follow columnar growth, there are subtle differences in the microstructure growth depending on whether they are classified as interstitial carbides or covalent carbides, which are influenced by the deposition temperature. Materials like TaC and HfC exhibit a mixed microstructure following the models of Van der Drift[13-15] and Structural Zone Model (SZM)[10], while SiC[20], although similar to columnar growth, has its own unique growth structure. Examining these growth structures in detail, depicted on Figure 2-7, the behavior following Van der Drift occurs in the following sequence:

1. In the early stages of nuclei formation, seed grains generate nuclei in arbitrary directions on the substrate (Incubation period).

2.The next stage is dominated by competitive growth among grains with random orientations.

3. As the film thickens, an increasing number of crystal nuclei become buried by adjacent crystal nuclei.

4. Only crystals with the fastest-growth-direction perpendicular to the substrate surface survive.

5. Formation of fibrous textures (Columnar-like structure).

and microstructural growth occurs in a pattern similar to Figure 2-7 and 2-8. In contrast, for SiC, as shown in Figure 2-9 and proposed by Chin et al[20], the growth model is followed, and the morphological changes in the microstructure are known to be significantly influenced by the deposition temperature.

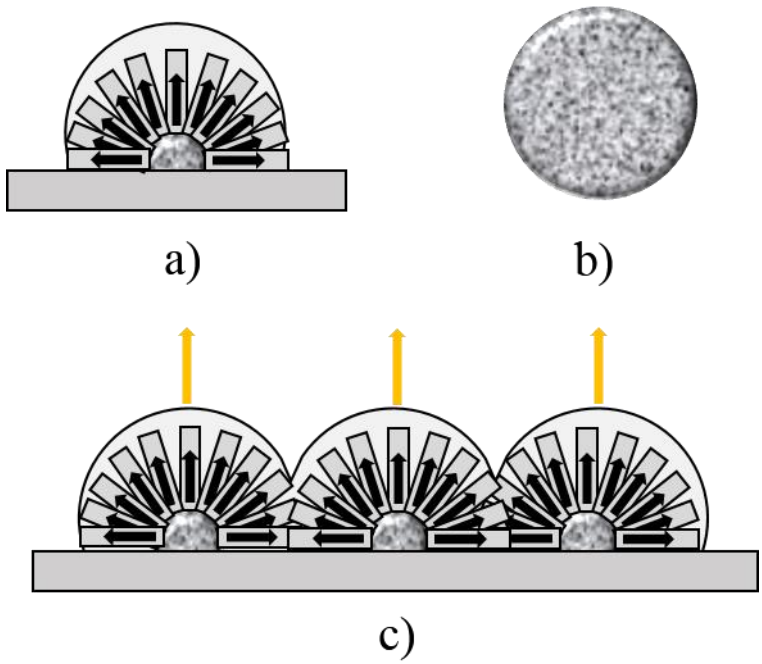

Figure 2-4. Growth model following Van der Drift model. a) initial single grain growth following Drift model (cross-section view), b) initial single grain growth following Drift model (Top view), c) Grain coalescence during deposition process.

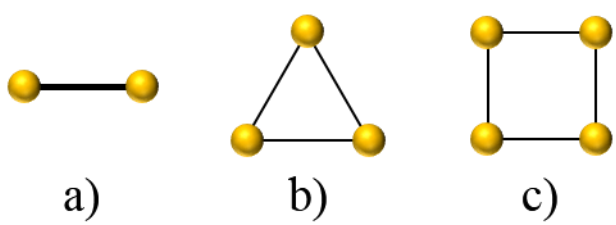

Figure 2-5. Nuclei types for atomistic growth. a) line-type nuclei, b) triangle-type nuclei, c) square-type nuclei.

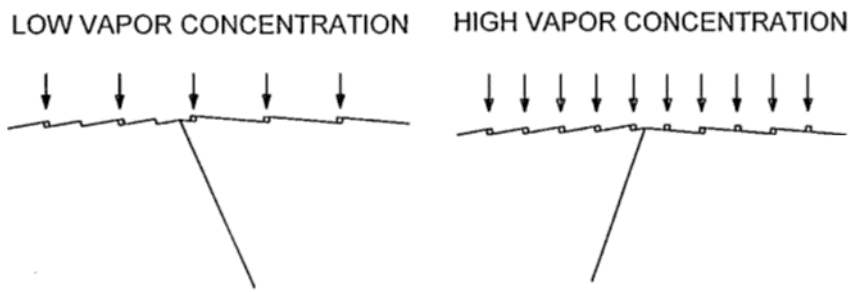

Figure 2-6. Surface energy formation by the different vapor concentrations [19].

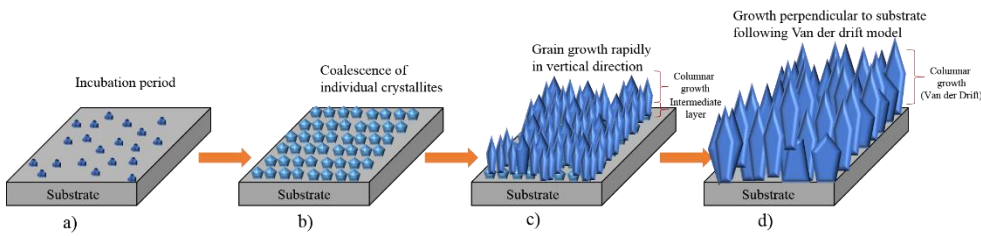

Figure 2-7. Film growth sequence following Drift model. a) initial nucleation state, seed crystal formation on the substrate, b) competitive growth of random oriented grains, c) columnar-like growth getting thicker, d) Fibrous texture structure.

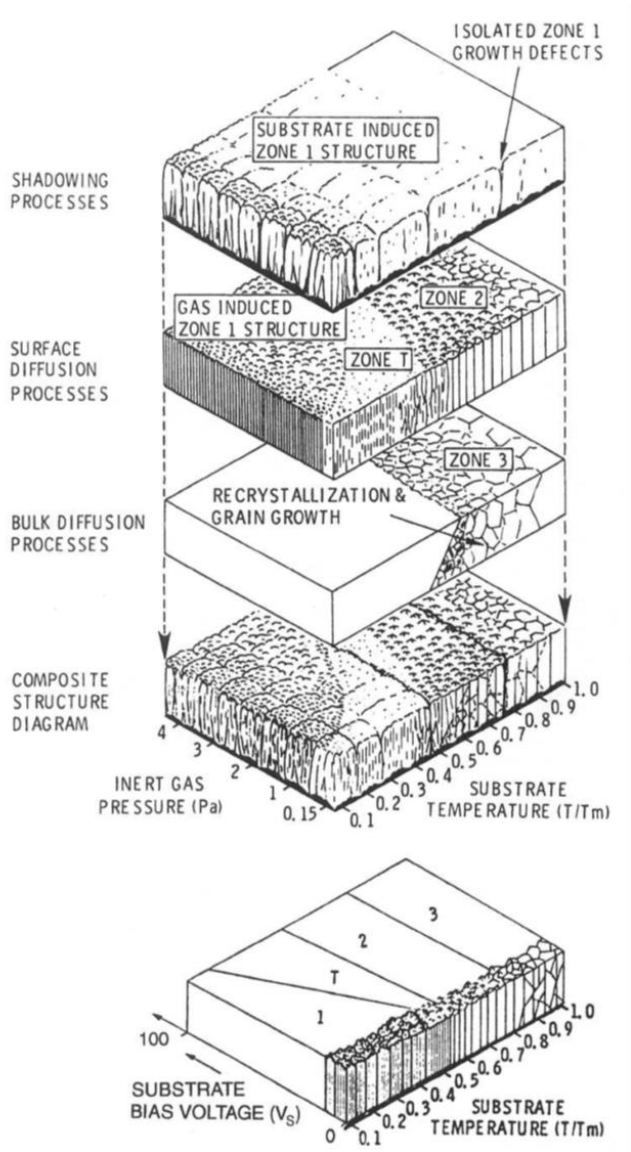

Figure 2-8. Structural Zone Model (SZM) of vapor depositions[10]

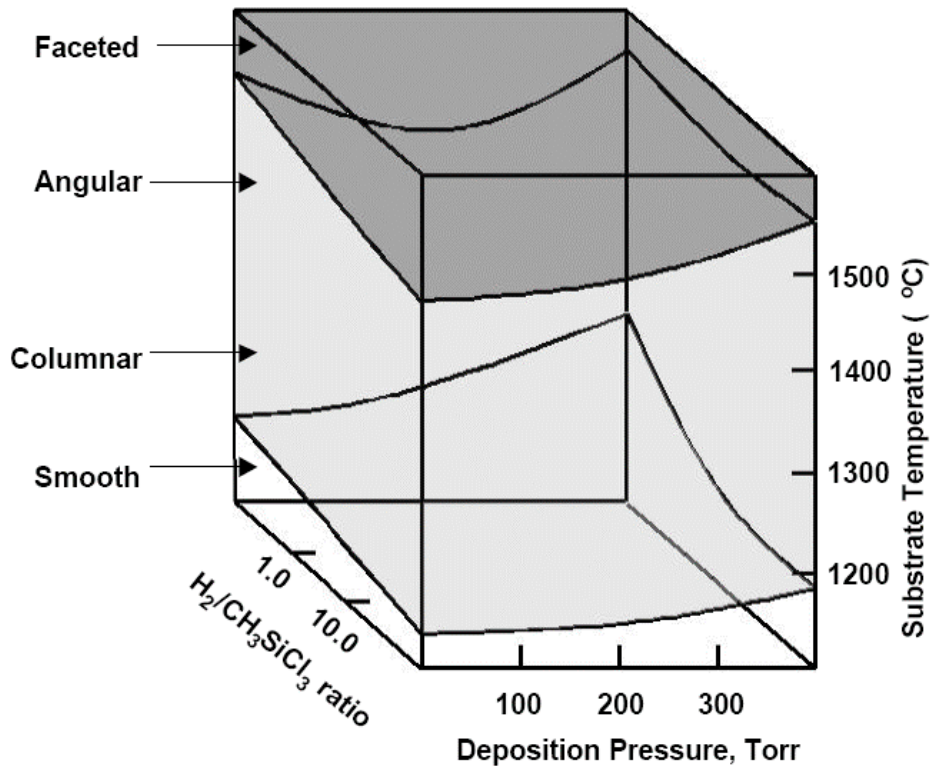

Figure 2-9. The relationship of morphology and deposition variables of SiC[20].

2.2.1 Tantalum carbide (TaC)

Tantalum carbide (TaC) is one of the refractory metal carbides with good performance in ultra-high temperature regions by their good thermomechanical properties. TaC is a one of the interstitial carbides with face-centered cubic (FCC) structure with complex phase diagram (Figure2-10) and extremely high melting point (approximately 3900ºC)[7-8], high modulus (537 GPa), high hardness (15-19GPa), flexural strength (689GPa), and good resistance to chemical attack[21-25]. Normally, TaC coating layers show brown to gold colors by the difference on carbon deficiency[25].

TaC is fabricated in the form of a sintered body[21-22] or deposited as a coating layer using high temperature CVD method (above 2000ºC)[7]. However, there are many ongoing studies to change the precursor and lower the process temperature[23-26], aiming to fabricate the coating layer in the form of fiber-reinforced composites[23]. TaC is widely applied in high temperature applications that are sensitive to chemical attack rather than requiring high oxidation resistance since oxidation starts rapidly from 800°C when exposed to air[7]. Particularly, recently it is used in the coating layer of ceramic susceptors used in wafer processing for semiconductor fabrication (Figure 2-11).

During the deposition process or consolidation using powders, there is a high probability of secondary phases such as Ta_2C and Ta_4C_3 forming[26-28]. The crystal structure in such cases is known to have forms like hexagonal close-packed (HCP) or tetragonal[7-8].

The microstructure and orientation are significantly influenced by $TaCl_5$ partial pressure and temperature during the deposition process[24]. Increase of deposition temperature leads to random orientations[25-26]. Also, with the higher $TaCl_5$ partial pressures orientation seems to be random with columnar-like microstructure on the cross section and pyramidal structures on the surface[25].

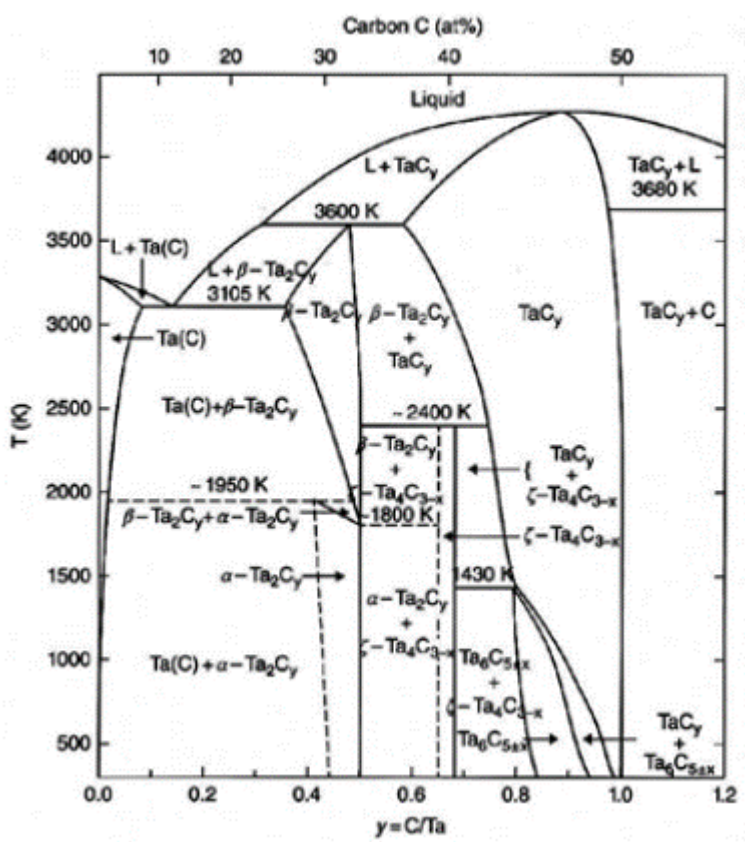

Figure 2-10. Phase diagram of Tantalum carbide (TaC)[7-8].

(a) (b) (c)

Figure 2-11. Ceramic susceptors for semiconductor process. (a) Instrument for semiconductor process; https://www.mersenkorea.co.kr (b) Graphite susceptor; TCK, susceptor, (c) TaC coated susceptor; TCK, susceptor.

2.2.2 Hafnium carbide (HfC)

Hafnium carbide (HfC) is a transition metal carbide in which the large metal atoms of hafnium form an FCC structure with small carbon ions occupying interstitial positions[7]. HfC exhibits certain characteristics typical of ceramics, as well as some characteristics more commonly associated with metals. The phase diagram of Hf-C is relatively simple (Figure 2-12). In this experiment, the HfC coating layers displayed a metallic silver-gray appearance and demonstrated good adhesion to graphite and carbon/SiC fiber preforms[7].

When HfC is produced as a sintered body, it exhibits high density, crystallinity, and excellent mechanical properties[29-30]. However, most applications require HfC to be manufactured in the form of fiber-reinforced composites[31-35]. HfC demonstrates high crystallinity and mechanical properties when deposited at temperatures above 1400°C. It is challenging to produce a dense microstructure coating layer even at low deposition temperatures. Additionally, variations in reaction temperature, reaction equation, and residual substances occur depending on the carbon source precursor, either C_3H_6 or CH_4[31-33]. To address these issues, there have been numerous studies which reported co-deposition of HfC with ZrC or TaC, among others[32-35].

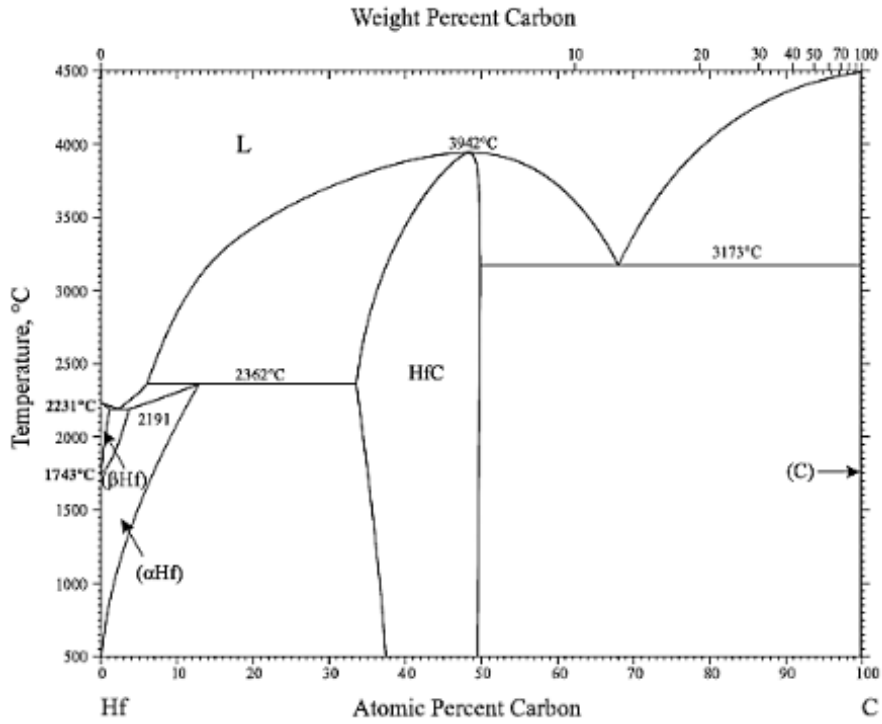

Figure 2-12. Phase diagram of Hafnium carbide (HfC)[7-8].

2.2.3 Silicon carbide (SiC)

Silicon carbide (SiC) is a material that has been studied for decades, and as a result, there is a significant amount of research being conducted. However, challenges still persist when applying SiC to fiber-reinforced type composites, such as fiber damage, residual stress at interfaces of interphase layer and coating layers, and variations in mechanical strength due to crystallinity[36-37].

SiC is a chemically and thermally stable material with strong covalent bonding, especially at high temperatures[7,20,36]. Figure 2-13 shows the Si-C phase diagram[38]. It can be divided into two main crystallographic structures: hexagonal in the form of type α-SiC, which includes 4H (Hexagonal), 6H (Hexagonal) and 15R (Rhombohedral), and cubic in the form of type β-SiC, as 3C (Cubic). 3C, 4H, 6H, and 15R being the most commonly used. The preferred form used as a structural material is type β-SiC with a 3C structure[36].

SiC has been widely used as a refractory material due to its excellent mechanical and thermal stability, including high hardness, flexural strength, compressive strength, nuclear properties, and oxidation resistance. It is extensively studied and developed as a structural material for ceramic engines, nozzles, and turbine blades, primarily due to its exceptional wear resistance and chemical stability.

Among them, chemical vapor deposition (CVD) is a technique that allows for the deposition of dense and high purity SiC, closely matching the theoretical density of 3.21g/cm^3. CVD enables uniform deposition over a large area, making it a commonly

used technique in coating processes. The microstructure of CVD SiC is influenced by process variables such as deposition temperature, process pressure, and gas ratio. The microstructure of CVD SiC is found to vary significantly depending on the deposition temperature, rather than the process pressure and input-gas-ratio. Therefore, by adjusting the process pressure and input-gas-ratio at a fixed deposition temperature, it is possible to predict the changes in microstructure.

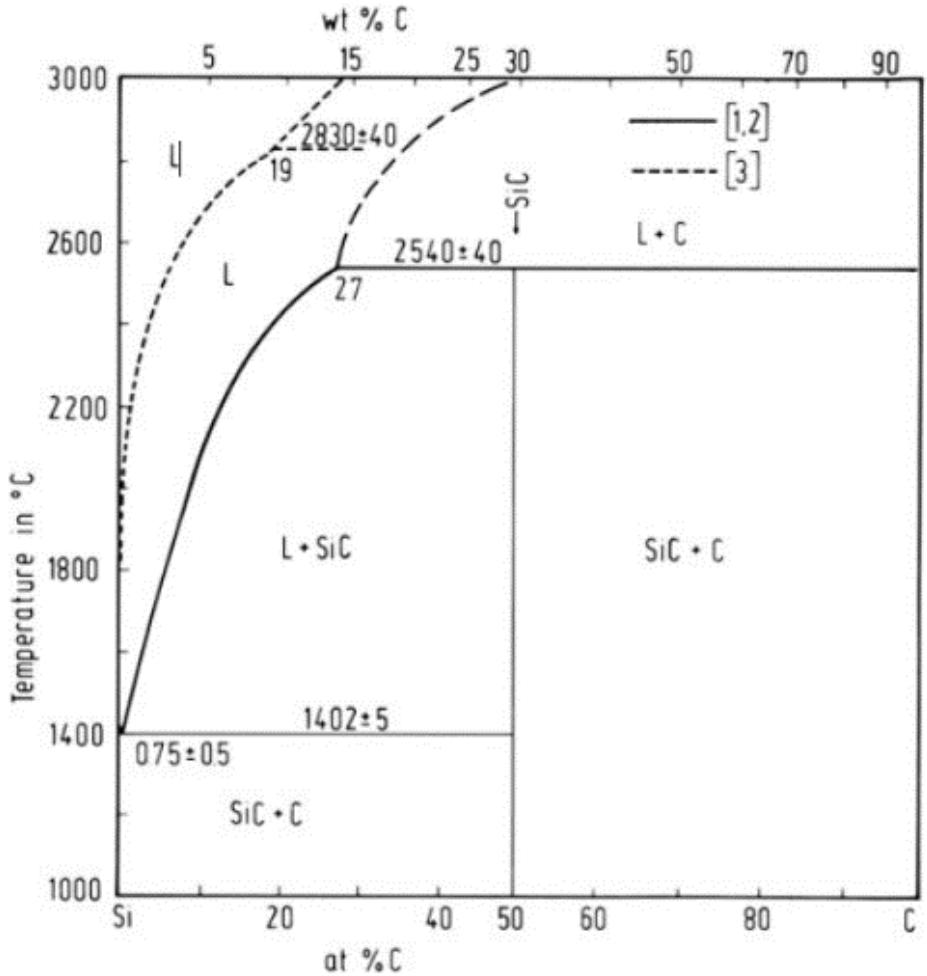

Figure 2-13. Phase diagram of Silicon carbide (SiC)[38].

2.3 Post-annealing process

The post-annealing process is commonly employed to relieve residual stress[39], mitigate thermal stress[40], reduce porosity to achieve densification[40-41], promote grain growth[41-44], enhance bonding strength[39-40,44,47], and induce crystallization in amorphous phases of the deposited thin films[42-43,46]. As a result, various outcomes such as increased peak intensity in XRD results[40-47], microstructural evolution, and improved mechanical properties can be obtained. In cases where the film contains amorphous phases, the crystallization and XRD peak intensity lead to an increase in the I/I0 ratio compared to the as-deposited state. Additionally, in certain material states, post-annealing may trigger atomic migration or diffusion[39,44,47], leading to phase transitions[47], where the post-annealing temperature serves as the driving force for the migration.

However, if the post-annealing temperature becomes excessively high, severe grain growth can occur, leading to rapid pore closure. This phenomenon can affect the bonding strength of the material[40], resulting in a decrease in mechanical properties due to microstructural changes[40,45]. Therefore, to improve the material properties, it is important to set a certain temperature range for the post-annealing process.

2.4 References

1. M. M. Opeka, I. G. Talmy, J. A. Zaykoski, *Oxidation-based materials selection for 2000◦C + hypersonic aerosurfaces: Theoretical considerations and historical experience*, J. Mater Sci., 39 (2004) 5887–5904

2. A. Paul, S. Venugopal, J.G.P. Binner, B. Vaidhyanathan, A.C.J. Heaton, P.M. Brown, *UHTC–carbon fibre composites: Preparation, oxyacetylene torch testing and characterization*, J. Eur. Ceram. Soc., 33 (2013) 423–432

3. William G. Fahrenholtz, Greg E. Hilmas, *Ultra-high temperature ceramics: Materials for extreme environments*, Scripta Mater., 129 (2017) 94–99

4. E. Wuchina, E. Opila, M. Opeka, W. Fahrenholtz, I. Talmy, *UHTCs: Ultra-High Temperature Ceramic Materials for Extreme Environment Applications*, Electrochem. Soc. Interface 16(4) (2007)

5. A. Sayir, *Carbon fiber reinforced hafnium carbide composite*, J. Mater. Sci., 39 (2004) 5995–6003

6. S. Tang, C. Hu, Design, *Preparation and Properties of Carbon Fiber Reinforced Ultra-High Temperature Ceramic Composites for Aerospace Applications: A Review*, J. Mater. Sci. Technol., 33 (2017) 117–130

7. H. O. Pierson, *Handbook of Chemical Vapor Deposition (CVD) Principles, Technology, and Applications*, NOYES PUBLICATIONS (1999)

8. G.B. Thompson, C.R. Weinberger, *Ultra-High Temperature Ceramics: Materials for Extreme Environment Applications*, John Wiley & Sons (2014)

9. W. A. Bryant, *The fundamentals of chemical vapour deposition*, J. Mater. Sci., 12 (1977) 1285-1306

10. M. Ohring, *Materials Science of Thin films*, Academic Press (2002)

11. E. Bauer, J.H. van der Merwe, *Structure and growth of crystalline superlattices: From monolayer to superlattice*, Phys. Rev. B, 33 (1986) 3657-3672

12. S. Barrat, P. Pigeat, E. Bauer-Grosse, *Three-dimensional simulation of CVD diamond film growth*, Diam. Relat. Mater., 5 (1996) 276 280

13. Z. Chen, Y. Zhuo, R. Hu,W. Tu, Y. Pei, B. Fan, C. Wang, G. Wang, *Control of morphology and orientation for textured nanocrystalline indium oxide thin film: A growth zone diagram*, Mater. Des., 131 (2017) 410-418

14. L. Krishnia, P. K. Tyagi, Growth and characterization of polycrystalline diamond films on silicon using sugarcane bagasse as carbon precursor at atmospheric pressure by thermal chemical vapor deposition, Diam. Relat. Mater., 87 (2018) 18-26

15. F. Silva, F. Be´ne´dic, P. Bruno, A. Gicquel, *Formation of <110> texture during nanocrystalline diamond growth: an X-ray diffraction study*, Diam. Relat. Mater., 14 (2005) 398–403

16. S. Stoyanov, *On The Atomistic Theory of Nucleation Rate*, Thin Solid Films 18 (1973) 91-98

17. V. Halpern, *A theory of orientation effects in nucleation on a crystalline substrate*, Brit. J. Appl. Phys. 18 (1967) 163-173

18. J. Pelleg, L.Z. Zevin, S. Lungo, N. Croitoru, *Reactive-sputter-deposited TiN films on glass substrates*, Thin Solid Films 197 (1991) 117-128

19. D. N. Lee, *Textures and related phenomena*, The National Academy of Engineering of Korea (2006)

20. J. Chin, P. K. Gantzel, R. G. Hudson, *The Structure of Chemical Vapor Deposited Silicon Carbide*, Thin Solid Films 40 (1977) 57–72

21. X. Zhang, G. E. Hilmas, W. G. Fahrenholtz, D. M. Deason, *Hot Pressing of Tantalum Carbide With and Without Sintering Additives*, J. Am. Ceram. Soc., 90 [2] (2007) 393–401

22. L. Liu, F. Ye, Y. Zhou, *New route to densify tantalum carbide at 1400 ◦C by spark plasma sintering*, Mater. Sci. Eng. A, 528 (2011) 4710–4714

23. C. Z.-Ke, X. Xiang, L. G.-Dong, S. Wei, L. Ying, *Texture structure and ablation behavior of TaC coating on carbon/carbon composites*, Appl. Surf.e Sci., 257 (2010) 656–661

24.Z.-K. Chen, X. Xiong, Y. Long, *Influence of $TaCl_5$ partial pressure on texture structure of TaC coating deposited by chemical vapor deposition*, Appl. Surf. Sci., 257 (2011) 4044–4050

25. X. Xiong, Z.-K. Chen, B.-Y. Huang, G.-D. Li, F. Zheng, P. Xiao, H.-B. Zhang,

Surface morphology and preferential orientation growth of TaC crystals formed by chemical vapor deposition, Thin Solid Films 517 (2009) 3235–3239

26. D. Kim, S. M. Jeong, S. G. Yoon, C. H. Woo, J. I. Kim, H.-G. Lee, J. Y. Park, W.-J. Kim, *Chemical Vapor Deposition of Tantalum Carbide from $TaCl_5$-C_3H_6-Ar-H_2 System*, J. Korean Ceram. Soc., 53 (2016) 597–603

27. B. Wang, N. De Leon, C. R. Weinberger, G. B. Thompson, *Theoretical investigation of the slip systems of Ta_2C*, Acta Mater. 61 (2013) 3914–3922

28. A.I. Gusev, A.S. Kurlov, V.N. Lipatnikov, *Atomic and vacancy ordering in carbide ζ-Ta_4C_{3-x} ($0.28<<x<<0.40$) and phase equilibria in the Ta–C system*, J. Solid State Chem., 180 (2007) 3234–3246

29. E. Wuchina, M. Opeka, S. Causey, K. Buesking, J. Spain, A. Cull, J. Routbort, F. Guitierrez-Mora, *Designing for ultrahigh-temperature applications: The mechanical and thermal properties of HfB2,HfCx, HfNx and αHf(N)*, J. Mater. Sci., 39 (2004) 5939–5949

30. A. Sayir, *Carbon fiber reinforced hafnium carbide composite*, J. Mater. Sci., 39 (2004) 5995–6003

31. Y.-L. Wang, X. Xiong, X.-J. Zhao, G.-D. Li, Z.-K. Chen, W. Sun, *Structural evolution and ablation mechanism of a hafnium carbide coating on a C/C composite in an oxyacetylene torch environment*, Corros. Sci., 61 (2012) 156–161

32. J. Ren, Y. Zhang, P. Zhang, T. Li, H. Hu, *UHTC coating reinforced by HfC*

nanowires against ablation for C/C composites, Surf. Coat. Tech., 311 (2017) 191–198

33. Y.-L. Wang, X. Xiong, G.-D. Li, H.-B. Zhang, Z.-K. Chen, W. Sun, X.-J. Zhao, *Microstructure and ablation behavior of hafnium carbide coating for carbon/carbon composites*, Surf. Coat. Tech., 206 (2012) 2825–2832

34. Y.-L. Wang, X. Xiong, G.-D. Li, H.-F. Liu, Z.-K. Chen, W. Sun, X.-J. Zhao, P*reparation and ablation properties of Hf(Ta)C co-deposition coating for carbon/carbon composites*, Corros. Sci., 66 (2013) 177–182

35. X. Xiong, Y.-L. Wang, G.-D. Li, Z.-K. Chen, W. Sun, Z.-S. Wang, *HfC/ZrC ablation protective coating for carbon/carbon composites*, Corros. Sci., 77 (2013) 25–30

36. A. Ivekovi´c, S. Novak, G. Dra˘zi´c, D. Blagoeva, S. Gonzalez de Vicente, *Current status and prospects of SiCf/SiC for fusion structural applications*, J. Eur. Ceram. Soc., 33 (2013) 1577–1589

37. H. Cheng, R. Tu, S. Zhang, M. Han, T. Goto, L. Zhang, *Preparation of highly oriented β-SiC bulks by halide laser chemical vapor deposition*, J. Eur. Ceram. Soc., 37 (2017) 509–515

38. V. Haase, G. Kirschstein, H. List, S. Ruprecht, R. Sangster, F. Schröder, W. Töpper, H. Vanecek, W. Heit, J. Schlichting, H. Katscher, *The Si-C Phase Diagram*, Springer (1985)

39. F. Wang, C. Zhang, X. Yan, L. Deng, Y. Lu, M. Nastasi, B. Cui, *Microstructure-Property Relation in Alumina Ceramics during Post-Annealing Process after Laser Shock Processing*, J. Am. Ceram. Soc., 101 (2018) 4933-4941

40. L. Zhao, F. Zhang, L. Wang, Shu Yan, J. He, F. Yin, *Effects of post-annealing on microstructure and mechanical properties of plasma sprayed Ti-Si-C composite coatings with Al addition*, Surf. Coat. Tech., 416 (2021) 127164

41. J.-H. Kim, M. Seo, S. Kang, *Effect of carbide particle size on the properties of W–ZrC composites*, Int. J. Refract. Met. Hard Mater., 35 (2012) 49–54

42. E. Colombini, M. Lassinantti Gualtieri, R. Rosa, F. Tarterini, M. Zadra, A. Casagrande, P. Veronesi, *SPS-assisted Synthesis of SICp reinforced high entropy alloys: reactivity of SIC and effects of pre-mechanical alloying and post-annealing treatment*, Powder Metall., 61 (2018) 64-72

43. Z. Li, P. Zhao, T. Lu, K. Feng, Y. Tong, B. Sun , N. Yao, Y. Xie , B. Han, X. Zhang, S. Tu, *Effects of post annealing on the microstructure, precipitation behavior, and mechanical property of a $(CoCrNi)_{94}Al_3Ti_3$ medium-entropy alloy fabricated by laser powder bed fusion*, J. Mater. Sci. Technol., 135 (2023) 142–155

44. F. Zhang, S. Yan, C. Li, Y. Ding, J. He, F. Yin, *Synthesis and characterization of MAX phase Cr_2AlC based composite coatings by plasma spraying and post annealing*, J. Eur. Ceram. Soc., 39 (2019) 5132–5139

45. B. Suleiman, H. Zhang, Y. Ding, Y. Li, *Microstructure and mechanical properties*

of cold sintered porous alumina ceramics, Ceram. Int., 48 (2022) 13531–13540

46. F. Zhang, J. Chen, S. Yan, G. Yu, H. Ma, J. He, F. Yin, *Microstructure and reaction mechanism of Ti-Al-C based MAX phase coatings synthesized by plasma spraying and post annealing*, Surf. Coat. Tech., 441 (2022) 128584

47. L. Wang, F. Zhang, S Yan, G. Yu, J. Chen, J. He, F. Yin, *Microstructure evolution and mechanical properties of atmosphere plasma sprayed AlCoCrFeNi high-entropy alloy coatings under post-annealing*, J. Alloy. Compd., 872 (2021) 159607

Chapter 3. Current issues of high temperature carbides

Research efforts are focusing on synthesis, processing, improving the oxidation resistance, design for extreme environments, adoption on fiber-reinforced composite types, computational simulations, and new materials development.

3.1 Processing temperature adjustment

Figure 3-1 shows the current issues of high temperature ceramic carbides. When examining the current issues, there appear to be four major issues. These include methods to enhance the properties of the coating layer or bulk by manipulating variables in the manufacturing process, methods to improve oxidation resistance, simulations for designing shapes and structures suitable for extreme environments, and issues related to developing new materials. In particular, controlling the process temperature is a significant consideration due to its economic impact. There are three main approaches to adjusting the process temperature: modifying the carbon source gas used in carbide materials to vary the process temperature, controlling the substrate temperature using the filament method, and simply adjusting the process temperature.

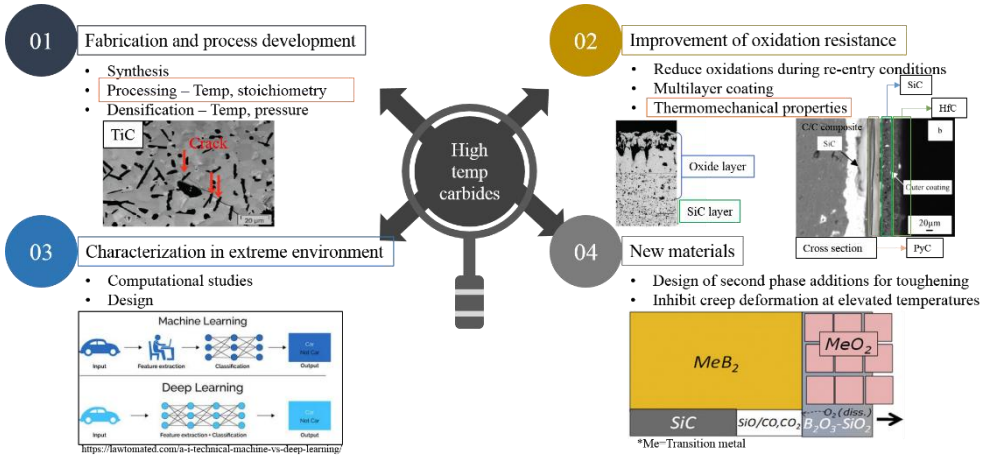

Figure 3-1. Current issues for high temperature ceramic carbides[1-5]

3.1.1 Effect of the carbon source gas

The process temperature can be adjusted by controlling the carbon source gas. As shown in Figure 3-2, it is possible to lower the temperature by replacing CH_4 gas, which decomposes above 1400°C, with C_3H_6, which can decompose below 1300°C[6-7]. However, reducing the temperature also reduces crystallinity, and complete decomposition of C_3H_6 can leave residual carbon in the fine structure of the coating layer, compromising its mechanical properties. Additionally, as shown in Figure 3-3, changing the carbon source gas can lead to the differentiation of fine structures into mixed and columnar structures[6-7]. This indicates that the deposition mechanism is influenced by temperature, ultimately affecting the changes in the fine structure.

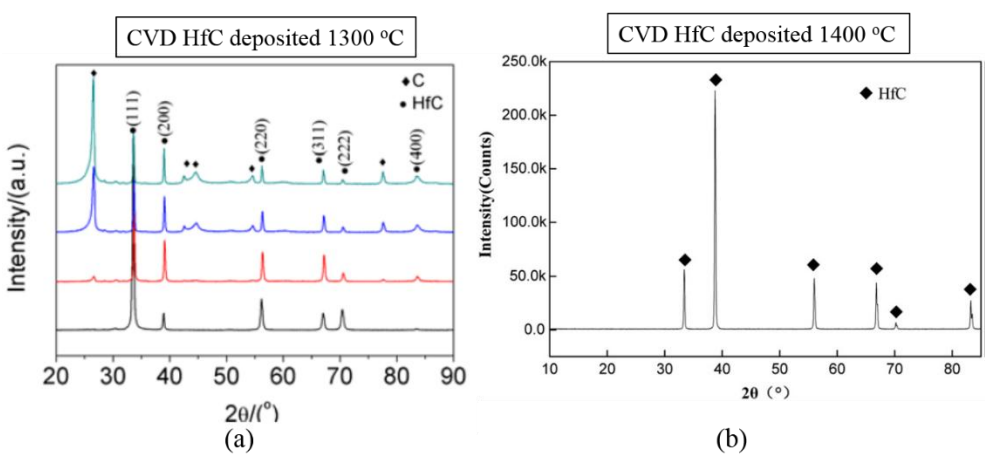

Figure 3-2. XRD results of HfC coating layers with different carbon source gas. (a) C_3H_6 gas, (b) CH_4 gas[6-7]

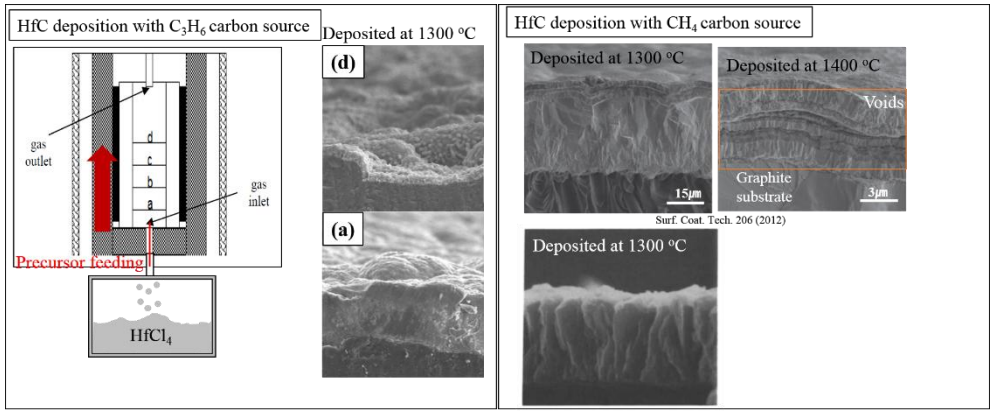

Figure 3-3. Effect of deposition temperature on the microstructure of HfC[6-7]

3.1.2 Effect of the deposition temperature

When the process temperature is lowered during manufacturing, regardless of the type of carbon source material, the crystallinity decreases, and carbon XRD peaks can be detected due to incomplete reactions. Furthermore, the influence of low temperature and partial pressure results in random orientation even at low deposition temperatures[8].

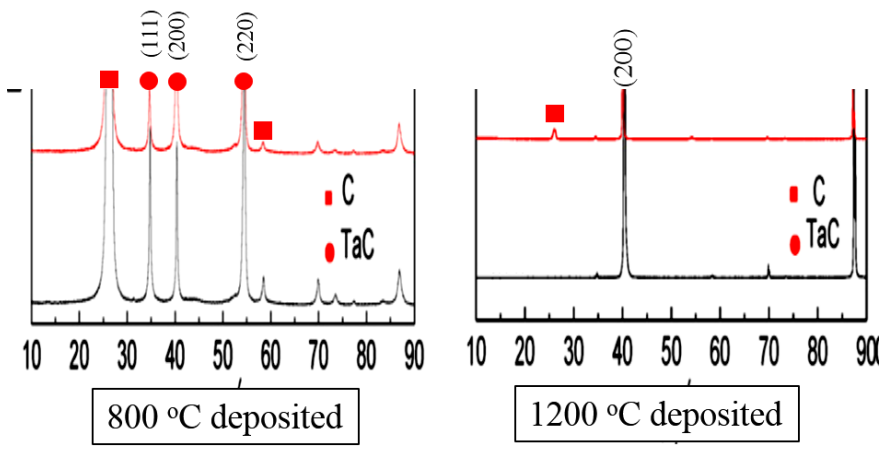

Figure 3-4. Changes in XRD patterns of high-temperature ceramic carbide coating layers at different deposition temperatures[8]

3.1.3 Filament CVD method

The Filament method using metal contributes to lowering the substrate temperature during the process, thus reducing the process temperature[9-11]. However, it has drawbacks such as the need to heat the metal filament at temperatures higher than those used in the CVD process, which can raise concerns regarding cost and safety.

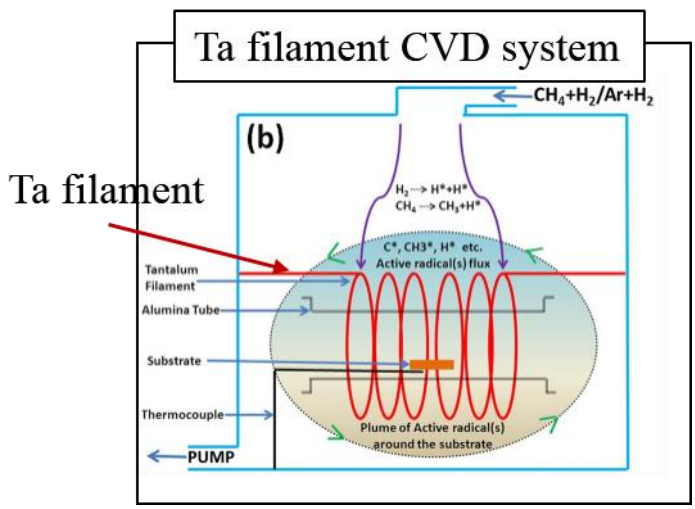

Figure 3-5. Schematic of filament CVD method[11]

Therefore, controlling the process temperature in the manufacturing of high-temperature ceramic carbide coatings has an impact on the crystallinity and fine structure of the resulting coatings. Moreover, these effects can influence the integrity of the coatings when applied in various applications, making it a crucial task to address.

3.2 References

1. M. M. Opeka, I. G. Talmy, J. A. Zaykoski, *Oxidation-based materials selection for 2000◦C + hypersonic aerosurfaces: Theoretical considerations and historical experience*, J. Mater. Sci., 39 (2004) 5887–5904

2. A. Paul, S. Venugopal, J.G.P. Binner, B. Vaidhyanathan, A.C.J. Heaton, P.M. Brown, *UHTC–carbon fibre composites: Preparation, oxyacetylene torch testing and characterization*, J. Eur. Ceram. Soc. 33 (2013) 423–432

3. William G. Fahrenholtz, Greg E. Hilmas, *Ultra-high temperature ceramics: Materials for extreme environments*, Scripta Mater., 129 (2017) 94–99

4. E. Wuchina, E. Opila, M. Opeka, W. Fahrenholtz, I. Talmy, *UHTCs: Ultra-High Temperature Ceramic Materials for Extreme Environment Applications*, Electrochem. Soc. Interface 16(4) (2007)

5. A. Sayir, *Carbon fiber reinforced hafnium carbide composite*, J. Mater. Sci., 39 (2004) 5995–6003

6. Y . Wang, H. Li, Q. Fu, H. Li, *Effect of deposition position on microstructure of HfC coating fabricated by low pressure chemical vapor deposition*, 18th International conference on composite materials (2011)

7. J. Ren, Y. Zhang, P. Zhang, T. Li, H. Hu, *UHTC coating reinforced by HfC nanowires against ablation for C/C composites*, Surf. Coat. Tech., 311 (2017) 191–198

8. Z.-K. Chen, X. Xiong, Y. Long, *Influence of $TaCl_5$ partial pressure on texture structure of TaC coating deposited by chemical vapor deposition*, Appl. Surf. Sci., 257 (2011) 4044–4050

9. M. Ali, M. Ürgen, M.A. Atta, *Tantalum carbide films synthesized by hot-filament chemical vapor deposition technique*, Surf. Coat. Tech., 206 (2012) 2833–2838

10. F. Togashi, K. Kobayashi, M. Mitsuhashi, S. Karasawa, S. Ohya, T. Watanabe, *Synthesis and morphology of CVD diamond on Ta and TaC film*, J. Cryst. Growth, 128 (1993) 418-424

11. R. Hawaldar, P. Merino, M. R. Correia, I. Bdikin, J. Grácio, J. Méndez, J. A. Martín-Gago, M. K. Singh, *Large-area high-throughput synthesis of monolayer graphene sheet by Hot Filament Thermal Chemical Vapor Deposition*, Scientific reports 2, 682 (2012) 00682

4. Experiments

In this chapter, experimental methods employed for the successful deposition and for the modification and characterization of high temperature carbide ceramics are presented. The coating layers in this study were deposited by chemical vapor deposition method, and to improve the crystallinity, microstructure, and evaluate the mechanical properties of the deposited coating layers, post-annealing process was performed. The characteristics of deposited coating layers were analyzed by X-ray diffractometer (XRD), microstructural evolutions of the deposited coating layers were observed by field-emission scanning electron microscopy (FE-SEM), and to evaluate the mechanical property of coating layer, nano-indentation method was carried out.

4.1 Chemical vapor deposition (CVD) methods

Chemical vapor deposition (CVD) is a method for depositing materials in which chemical components in vapor phase react to form a film or coating structures at various type of substrate surface. During the deposition process, it is necessary to maintain laminar flow in order for the deposition behavior to occur properly. If turbulent flow is maintained during the process, the deposition behavior will not occur properly, and a coating layer will not form on the substrate or fiber preform[1-

2].

In order for the chemical reaction to initiate the deposition process, the reactants need to be in a vapor state. Therefore, precursors used at this stage are typically subjected to evaporation processes if they are in powder form, or converted into vapor state if they are in liquid form. This is considered as a main factor for the chemical vapor deposition process[2].

The process sequence of CVD begins when the vapor state reactants start flowing into the furnace, initiating a series of processes. The reactants at this stage undergo a series of steps, eventually leading to the formation of a solid deposition through the process in a quasi-steady state. This sequence is illustrated schematically in Figure 4-1 with the following orders.

1. Diffusions of gaseous reactants by main flowing region

2. Adsorption of the reacting gas phase species on to surface region, often transport to surface area.

3. Surface chemical reactions occur by surface diffusion process.

4. Readsorption of the reaction by-products

5. Diffusion of the by-products away from the surface.

6. Incorporation of the condensed solid product into the microstructure of the growing film.

In this study, high temperature carbide ceramic coating layers (TaC, HfC and SiC) were deposited by CVD method.

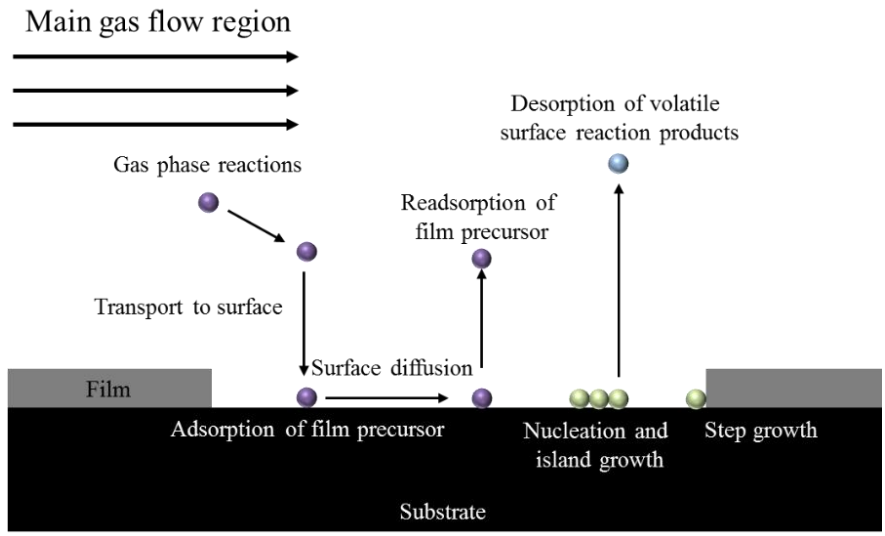

Figure 4-1. Gas phase reactions of precursors in the CVD furnace

4.2 Post-annealing process

Typically, operating temperatures higher than the temperature at which the material is used are harmful because it degrades the mechanical properties of the material[3]. Therefore, when the temperature of the heat treatment process performed on the material is higher than a certain reference point, the mechanical properties tend to decrease. However, if the material is heat-treated at a temperature suitable for diffusion, its mechanical properties can be improved without causing damage to the material. A heat treatment process with sufficient process time and temperature is called an annealing process. During annealing, materials tend to show changes in mechanical properties. This change is not a phase transition, but mainly a microstructural change. In addition, through annealing, the energy state of a material is changed from a metastable state to a stable state. When the post-annealing process is performed at an appropriate temperature rather than simply at an arbitrary high temperature, damage to the material can be reduced and mechanical properties will be effectively improved[3-7]. For that reason, finding an effective post-annealing temperature and conditions is very important for long-term use and the improvement of properties such as high-temperature stability and mechanical properties which are closely related to microstructure, crystallinity, residual stress, etc.

In this study we have performed post-annealing process on deposited coating layers. Detailed post-annealing conditions are presented on Table 4.1.

Table 4-1. Post-annealing conditions for coating layers.

	Temperature (°C)	Time (h)	Conditions
TaC	1850	5	Ar flowing
HfC	1600	10	Ar flowing
	1800	10	Ar flowing
SiC	800	10	Ar flowing
	1200	10	Ar flowing
	1500	10	Ar flowing

4.3 X-ray diffraction analysis

X-Ray diffraction analysis was performed to identify the original phases, orientation, and crystallinity change of the deposited coating layers after post-annealing. This method provides information about phase composition, lattice parameter, grain size, and lattice strain based on Bragg's law[8], where diffraction occurs when waves interact with a periodic structure. X-rays, with wavelengths similar to inter-atomic distances, are used to investigate crystals. Bragg's law is satisfied when waves interfere constructively under specific conditions.

$$n\lambda = 2d \sin\theta$$

Where n is an integer indicating the order of reflection, λ is the wavelength of the X-ray beam, d is the inter-planar spacing and θ is the incident angle. In the present work θ-2θ scans were performed using Bruker D8 discover (Bruker), SmartLab (Rigaku) diffractometer with Cu Kα radiation. In this geometry, the detector is at 2θ and the sample surface is at θ angle to the incident beam. The incident beam, normal to sample surface and detector are in the same plane (Figure 4-2). Since the diffracted beam always lies in the plane containing the incident beam and plane normal, and due to the restricted rotation of the sample only along θ-axis, this diffractometer can be used to access diffraction information only from the planes which are parallel to surface of the sample.

In the present study the Bruker D8 discover (Bruker), SmartLab (Rigaku) system was used to perform θ-2θ scans for phase identification and qualitative analysis of preferred orientation.

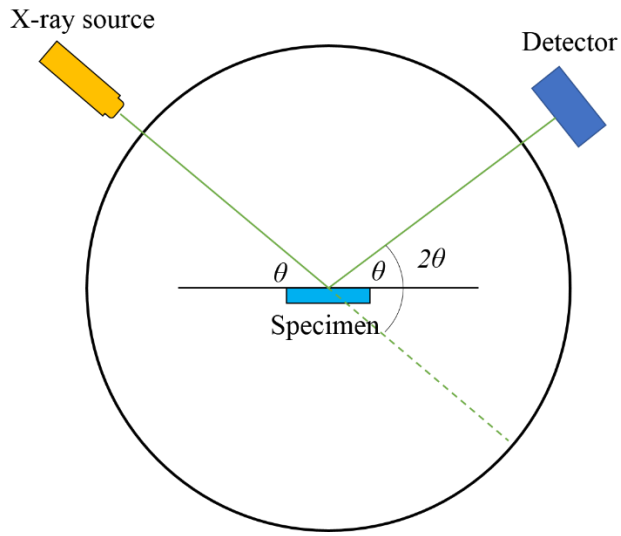

Figure 4-2. Schematic of typical X-ray diffraction instrument.

4.4 Microstructural observation

To observe the morphology of sintered bulk specimens or deposited thin film specimens, it is difficult to do so with the naked eye. Therefore, microscopy techniques such as scanning electron microscopy (SEM) using an electron beam are employed to detect the scattered electrons and observe the microstructure of the surface or cross-section. Various information about the specimen can be obtained through the incident electron beam, including Auger electrons, backscattered electrons, and cathode luminescence[8].

However, in conventional scanning electron microscopy, high-magnification observation is difficult due to the scattering of the electron beam during its interaction with the specimen. To improve the resolution of the electron beam, applying an electric field such as field-emission scanning electron microscopy to focus the electron beam at a single point can be more conveniently applied to observe the morphology of the surface.

In this study, we have observed the cross-section and surface microstructures of the deposited coating layers using a Field-Emission Scanning Electron Microscope (FE-SEM, FEI, Netherland) to examine the microstructure.

4.5 Nano-indentation measurements

Hardness is an important mechanical property that represents the resistance of a material to localized deformation. Hardness testing was developed as a method to assess the indentation depth of materials, particularly natural minerals. It involves applying a small load with a controlled rate of loading on the surface of a specimen using an indenter, in order to obtain quantitative measurements[8]. The depth or size of the indentation is inversely related to the hardness value, meaning that larger and deeper indentations correspond to lower hardness values. However, it should be noted that hardness measurements are relative rather than absolute, and caution should be exercised when comparing measurements obtained using different methods. The general advantages of hardness testing are as follows:

1. Compared to other mechanical property measurements, hardness testing is relatively simple and does not require a separate specimen preparation process.
2. It is a non-destructive testing method, meaning that the specimen is not destroyed or excessively deformed. However, surface or localized deformation in the form of indents may be observed.
3. Hardness values can be used to estimate other mechanical properties such as tensile strength through approximate formulas and calculations. However, these values are not exact and should be considered as calculated approximations.

These hardness values are easily measured when dealing with bulk specimens.

However, with the miniaturization of components and the inability to measure local areas, the demand for measurements such as nanoindentation has arisen[9]. In the case of macro hardness, a specified load is applied to the indenter in contact with the specimen, and after removing the load, the area of the residual impression is measured. The hardness value is obtained by dividing the load by the area. On the other hand, in the case of nano hardness, the depth of penetration is measured when a load is applied. The contact area within the total load is determined by the depth and known angle or radius of the indenter. Hardness is calculated by dividing the load by the contact area. The shape of the unloading curve provides a measure of the elastic modulus.

In this study we have used nano indentation method to measure the nano hardness of deposited coating layers by nano-indenter (CSM Instruments, U.S.A) with 10 points.

4.6 References

1. M. Ohring, *Materials Science of Thin films*, Academic Press (2002)

2. S. Sivaram, *Chemical vapor deposition: Thermal and Plasma Deposition of Electronic materials*, Van Nostrand Reinhold (1995)

3. H. Dong, X. Gao, S. Zhang, Y. Song, J. Yang, F. Wang, *Effects of heat treatment on the mechanical properties at elevated temperatures of plain-woven SiC/SiC composites*, J. Eur. Ceram. Soc., 42 (2022) 412–419

4. A. Udayakumar, A.S. Ganesh, S. Raja, M. Balasubramanian, *Effect of intermediate heat treatment on mechanical properties of SiCf/SiC composites with BN interphase prepared by ICVI,* J. Eur. Ceram. Soc., 31 (6) (2011) 1145–1153

5. X. Han, X.G. Gao, Y.D. Song, *Effect of heat treatment on the microstructure and mechanical behavior of SiC/SiC mini-composites*, Mater. Sci. Eng. A, 746 (2019) 94–104

6. H. Mei, H. Zhang, W.Z. Huang, M. Han, Y.W. Xu, L.F. Cheng, *Effects of heat treatment temperatures on microstructures and mechanical properties of the chopped carbon fibres SiC composites*, Adv. Appl. Ceram., 117 (7) (2018) 389–394

7. Korean ceramic society, *Handbook of high-tech ceramics*, Korean ceramic society (2007)

8. W. D. Callister, *Materials Science and Engineering an Introduction*, Wiley (2008)

9. Anthony C. Fischer-Cripps, *Introduction to Contact Mechanics*, Springer (2000)

Chapter 5. Chemical vapor deposition of ceramic carbides

High temperature ceramic carbides (TaC, HfC, SiC) were deposited by chemical vapor deposition with different deposition parameters. Carbide materials are identified by interstitial carbide and covalent carbide by its bonding structures. Tantalum carbide (TaC) and hafnium carbide (HfC) are referred as interstitial carbides, and silicon carbide (SiC) is referred as a covalent carbide. Deposited coating layers were characterized with X-ray diffraction (XRD) and cross-section microstructure observation.

5.1 Interstitial carbides

5.1.1 Tantalum carbide (TaC)

Tantalum carbide (TaC) was deposited on 2-inch diameter graphite substrate by using $TaCl_5$-C_3H_6-H_2 chemical vapor deposition method. Deposition was carried out at different temperatures (1100 – 1300 ºC). $TaCl_5$ (>99.99%, STREM CHEMICALS, U.S.A) powder and C_3H_6 gas (99.99%) were used as the source of Ta and carbon, respectively. The temperature of sublimation chamber and mixing heater was 240 ºC and 400 ºC, respectively for the complete reaction of $TaCl_5$ powders. Detailed deposition parameters are shown on Table 5.1

Figure 5-1 shows the XRD results of TaC coating layers deposited by the CVD

method at different deposition temperatures. The TaC coating layers exhibited different orientations depending on the deposition temperature. The coating layer deposited at 1100ºC showed a highly oriented (111) TaC peak, while at 1200ºC, it exhibited a highly oriented (200) TaC peak. Lastly, the XRD result at 1300ºC indicated random orientation of TaC. The reason why the (111) peak appears first is that, at lower deposition temperatures, it preferentially grows to reduce the surface energy of the forming coating layer. Similar results were observed in commercially available specimens deposited at temperatures above 2000ºC using the CVD method [1-2]. It was also reported that during the deposition process, variations in the partial pressure of $TaCl_5$ resulted in the formation of randomly oriented TaC[3]. The deposited coating layers generally exhibit a texture with respect to the film orientation. When deposited at low temperatures, the orientation of the peak changes from (111) to (200) due to the predominant influence of surface reaction kinetics and the lower surface energy on (111) [4-6].

TaC coating layers, deposited with different deposition temperatures, showed changes in the observed microstructure in cross-sectional SEM analysis as the deposition temperature was increased (Figure 5-2). The TaC coating layer deposited at 1100℃ (Figure 5-2 (a)) exhibited a microstructure similar to Zone 1, which has columnar structures, the microstructure of the low temperature region, as seen in the initial stated of Van der Drift model[7-10] and structural zone modeling (SZM)[11]. When the deposition temperature was increased, a mixed microstructure (or wave-like structure) with a combination of Zone 1 and Zone T which is similar to Van der drift model grown microstructures was observed (Figure 5-2 (b), (c)). The zone

modeling structure sequence works as Zone 1 (Columnar with pore structures)-Zone T (Fiber textured columnar structure)-Zone 2 (Dense columnar structures). This occurred as the mixed microstructure filled the region of pores that would typically be present in the low-temperature deposition microstructure, which is similar to a Zone 1 microstructure. In the microstructure of TaC coating layer deposited at 1300℃, this mixed microstructure was more pronounced, and the structure that resembled columnar structure was not observed. Similar observations of mixed microstructures of this nature were also reported in the results of Chen et al.[3] (Figure 5-3). The cross-sectional microstructure seems to be similar to the Zone 2 model, which is deposited at a relatively higher temperature than in this study. Also, the surface microstructures showed pyramidal structures, which follow the Van der Drift morphology[7-10]. These changes in the microstructure can be attributed to the formation of a mixed microstructure where equiaxed grains are located within the porous columnar structure that can be formed during low temperature deposition.

Table 5.1. Deposition conditions for chemical vapor deposited TaC coating layers ($TaCl_5$-C_3H_6-H_2 was used)

Deposition temperature (°C)	Deposition time (h)	Gas flow rate (sccm)	
		H_2	C_3H_6
1100	0.5	4900	100
1200	0.5	4900	100
1300	0.5	4900	100

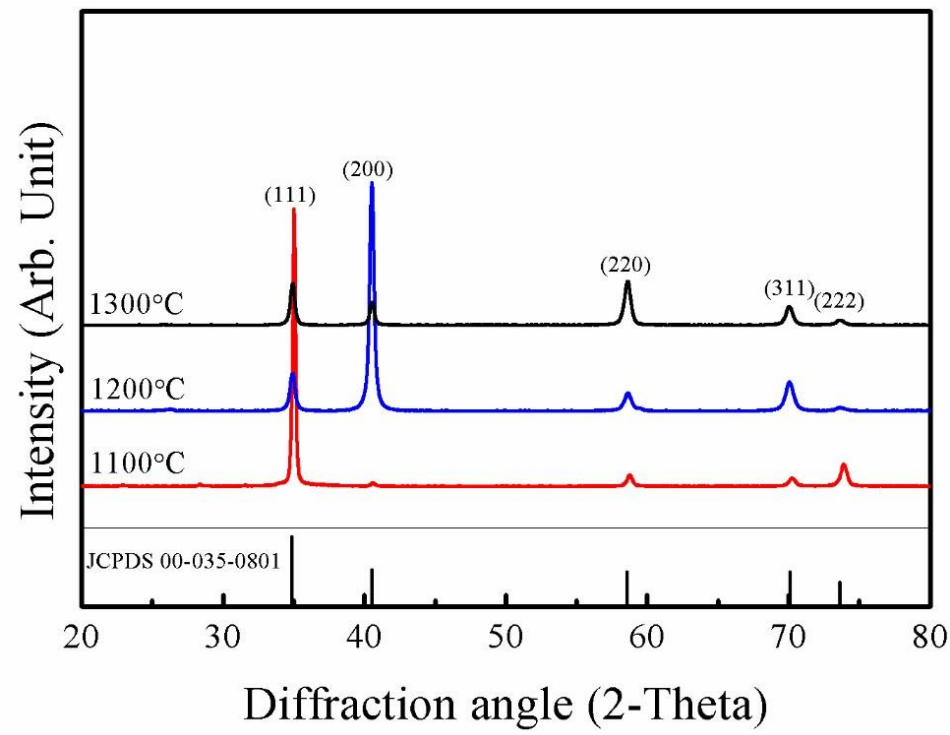

Figure 5-1. XRD results of TaC coating layers deposited at different temperatures show that as the deposition temperature increases, the peak orientation changes from (111) to (200) and becomes random.

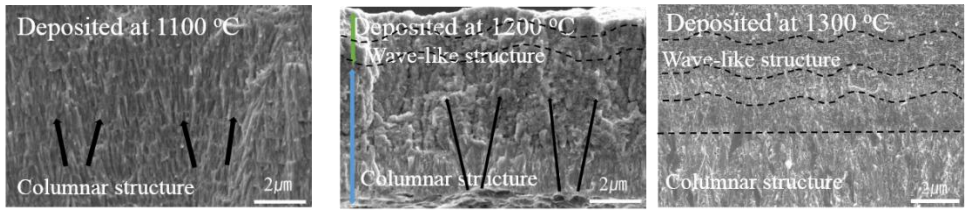

Figure 5-2. Cross-section microstructure of TaC coating layers deposited at (a) 1100°C, (b) 1200°C, and (c) 1300°C. The microstructures change from columnar to a mixed structure as deposition temperature is increased

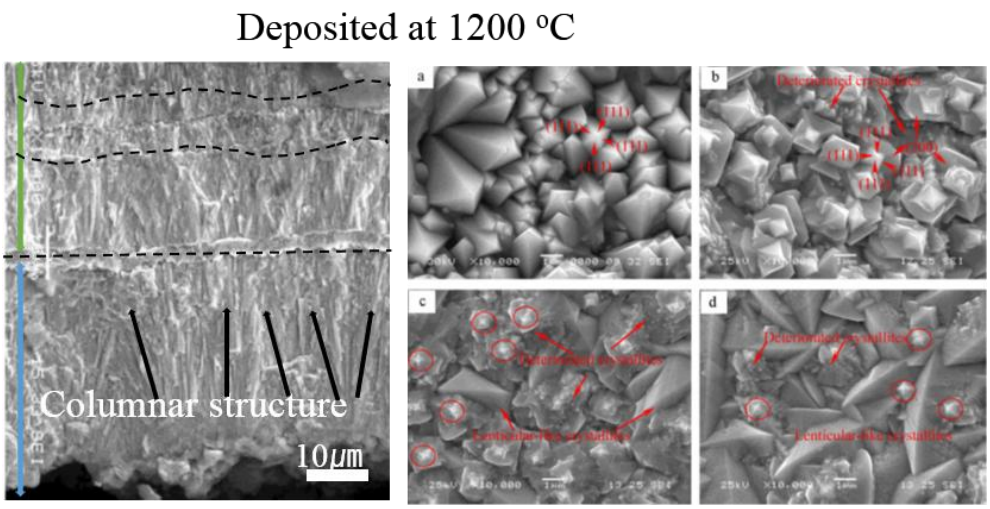

Figure 5-3. SEM images of TaC deposited at 1200°C which shows a mixed microstructure on the cross-section and a pyramidal shape on the surface (Chen et al)[3]

5.1.2 Hafnium carbide (HfC)

Hafnium carbide (TaC) was deposited on 2-inch diameter graphite substrate by $HfCl_4$-C_3H_6-H_2 chemical vapor deposition system. Deposition was carried out with different partial pressures at 1200ºC. $HfCl_4$ (>99.99%, STREM CHEMICALS, U.S.A) powder and C_3H_6 gas (99.99%) were used as the source of Hf and carbon, respectively. The temperature of both the sublimation chamber and the mixing heater was 300ºC for the complete reaction of $HfCl_4$ powders. The detailed deposition condition is shown in Table 5.2.

The X-ray diffraction (XRD) results of the HfC coating layer, deposited via the chemical vapor deposition (CVD) method, are presented in Figure 5-4. The XRD analysis confirmed the deposition of a single-phase HfC with random orientations. However, a significant amount of free carbon was observed. Such free carbon can have detrimental effects on the microstructure, mechanical behavior, and oxidation resistance. Therefore, it is necessary to control its presence. Consequently, by adjusting the partial pressure of $H_2/(HfCl_4+C_3H_6)$ during the deposition process, the peak attributed to free carbon was eliminated; however, it resulted in relatively low crystallinity. To enhance crystallinity and achieve a denser microstructure, the partial pressure was adjusted by reducing the amount of diluent gas, H_2. As a result, the XRD intensity values showed improvements in crystallinity compared to the previous results[12-13]. However, in the previous results, HfC coatings using CH_4 as carbon source gas seems to show higher XRD intensity in the results[12].

When observing the microstructure of HfC with a significant amount of detected

free carbon, the microstructure on the cross-section appeared dense (Figure 5-5). However, on the surface, a cauliflower-like microstructure was observed. By adjusting the partial pressure of $H_2/(HfCl_4+C_3H_6)$ during the deposition, a transformation of the microstructure from a cauliflower-like morphology to a nano-rod-like structure was observed. To achieve a dense microstructure diluent gas amount was adjusted, both the cross-section and the surface exhibited dense microstructures. Furthermore, the surface microstructure exhibited a pyramidal shape similar to the typical surface microstructure of the Drift model. The microstructure exhibited a similar pattern to the microstructure of TaC in SZM, where the microstructures of Zone 1 and Zone T were mixed, resembling the microstructure of Van der Drift model[7-10]. As seen in Figure 5-6, at low deposition temperatures, the microstructure appears to be columnar-like. However, as the deposition temperature increases, the structure seems to transition into mixed microstructures. Furthermore, by applying the temperature-dependent Van der Drift model[7-10], we can anticipate the following changes. At high partial pressures, the initial grain nuclei are expected to exhibit a shape close to cauliflower, but as the partial pressure changes, they gradually adopt a dense form.

Table 5.2 Deposition conditions for chemical vapor deposited HfC coating layers ($HfCl_4$-C_3H_6-H_2 was used)

Specimen	Deposition temperature (°C)	Deposition time (h)	Gas flow rate (sccm)	
			H_2	C_3H_6
H1	1200	0.5	3200	50
H2	1200	0.5	3200	10
H3	1200	0.5	800	10

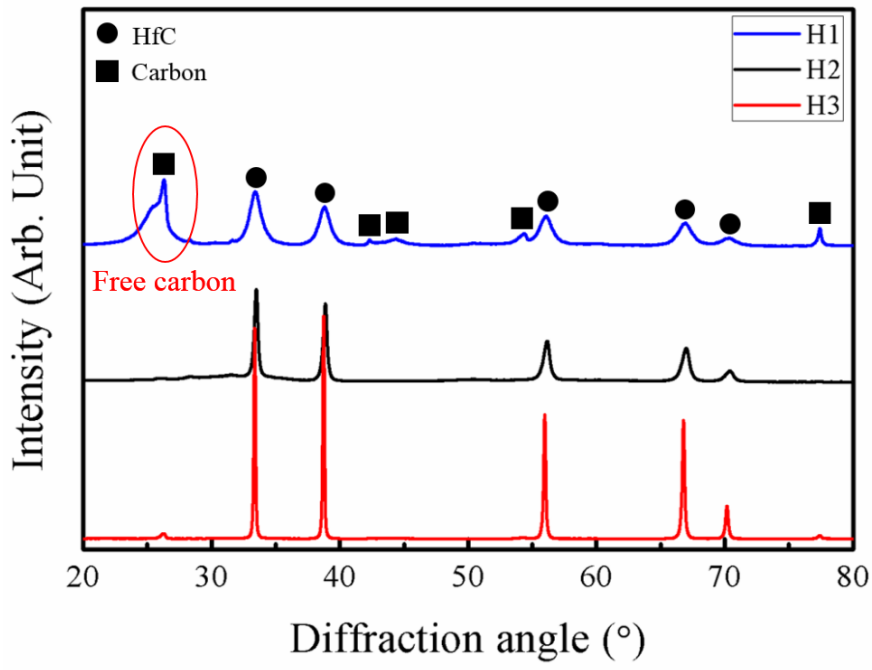

Figure 5-4. XRD results were obtained for HfC coating layers deposited under different deposition parameters.

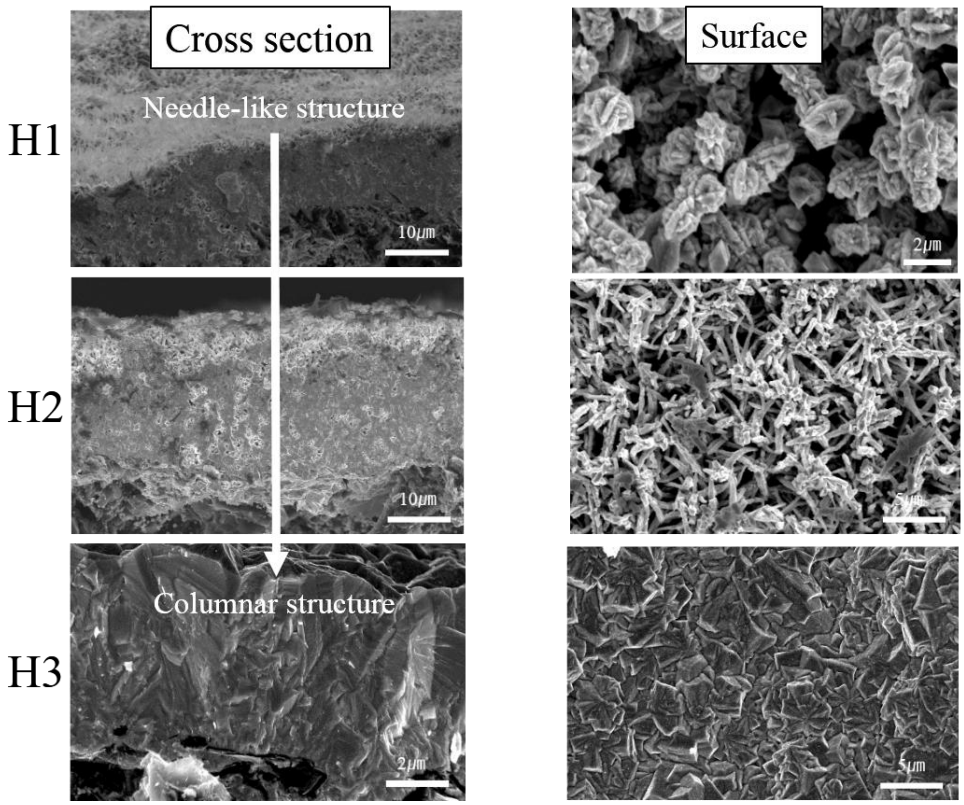

Figure 5-5. Microstructure analysis of HfC coating layers with different deposition parameters. H1: Needle-like structure (Cauliflower structure on surface), H2: Columnar-like structure (Nano-rod structure on surface), H3: Columnar-like structure (Dense faceted structure on surface).

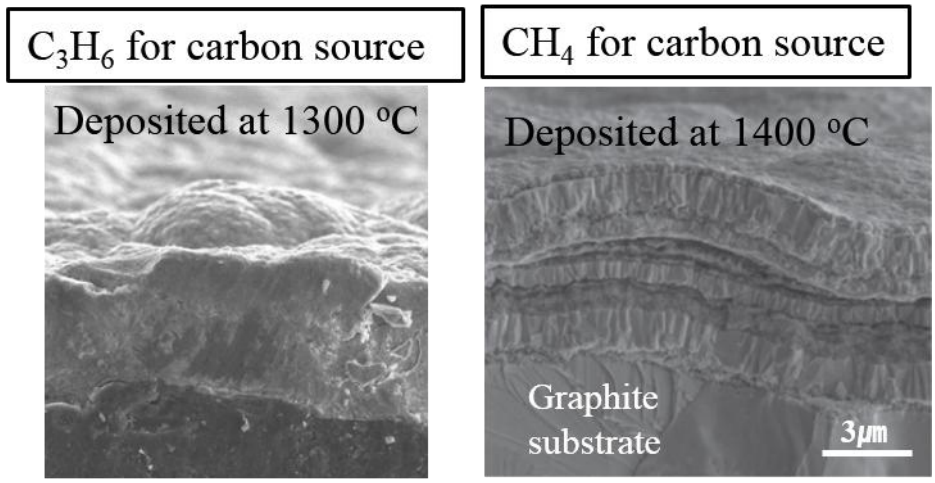

Figure 5-6. Cross-sectional microstructures of HfC coating layers deposited using different carbon sources (Ren et al, Wang et al) [13,15]

5.1.3 Growth mechanism of TaC and HfC coating layers based on Drift model

Unlike SiC, which has established CVD growth mechanisms and morphology maps [17], TaC and HfC, do not have proposed morphology maps. However, they can be explained using models such as Van der Drift's model [7-10] or the Structural Zone Model (SZM) [11,17], which exhibit similar growth behavior. The growth initiation, where reactants adsorb onto the substrate, resembles the island growth model. However, it then shows a growth pattern similar to the coexistence of Zone 1 and Zone T suggested by SZM. This can be more accurately depicted as the growth model shown in Figure 5-7. In contrast, SiC is mainly influenced by temperature among factors like partial pressure and input-gas ratio, and in most cases, the microstructure of the cross-section remains mostly columnar, with surface morphology changing according to temperature [17].

At the initial nucleation stage, seed crystals nucleate on the substrate with random orientation. The following stage is governed by the competitive growth between crystals with random orientation. As the film gets thicker, more and more grains are buried by adjacent grains. Only the crystals with the fastest growth direction normal to the substrate surface survive, resulting in the formation of a fiber texture.

In the case of TaC and HfC, the directionality of growth and the particle shape of the microstructure can be determined through two variables: temperature and precursor distribution. As the deposition temperature is increased, the growth direction is influenced by thermal conductivity (Figure 5-8), resulting in a growth direction closer to the vertical at lower temperatures. In this case, the growth

direction of the deposited coating layer or film is determined by the thermal stress applied during the process. Therefore, columnar-like microstructures are observed at lower temperatures. However, as the deposition temperature is increased, the growth direction becomes predominantly horizontal, following the direction of thermal conductivity or reducing surface energy [18]. When the precursor pressure is low, the particles on the surface exhibit a cauliflower-like shape or a nano-rod-like structure. On the other hand, as the precursor concentration is increased, particle growth occurs, and the microstructure of the coating layer becomes denser

Figure 5-9 and Figure 5-10 represent a morphological map that allows for growth prediction based on temperature and precursor pressure variables for the corresponding microstructures. By controlling the indicated variables, the shape and density of the microstructure can be adjusted.

As mentioned above, when TaC deposition process occurs at low temperatures, it tends to form a columnar structure with (111) orientation to reduce surface energy. However, as the process temperature increases, it follows the Drift model, and the growth direction is influenced by the major factor, evolutionary selection, or thermal conductivity. Consequently, the coating layer, which was growing perpendicular to the substrate, transitions to a horizontal growth direction due to the increase in deposition temperature.

In the case of HfC, when depositing the coating layer, the flow rate change, which alters the concentration of the precursor and diluent gas, had more influence on the density rather than the shape of the microstructure, compared to the variable of

deposition temperature. If temperature is considered as a variable, it is anticipated that, similar to the microstructure change in TaC following the Drift model, the columnar structure could evolve into a mixed structure.

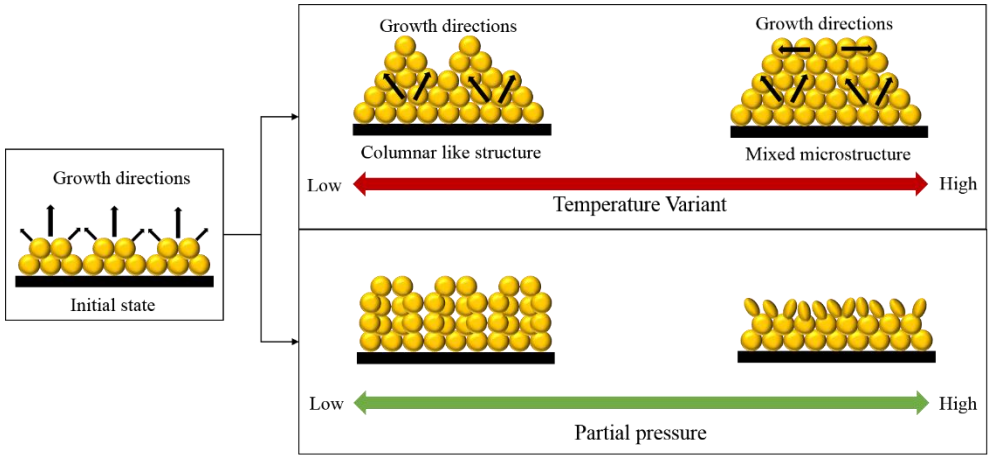

Figure 5-7. Growth model for interstitial carbide coating layers. The growth of this coating layer is determined by two variables, namely the deposition temperature and partial pressure (precursor concentration), and these two variables influence the growth of the coating layer.

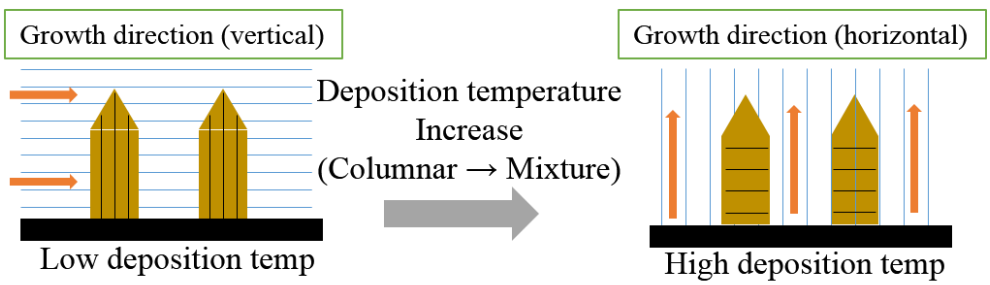

Figure 5-8. The effect of process temperature on the growth direction of the film is as follows: at low temperatures, the growth direction is vertical, while at high temperatures, the growth direction is horizontal.

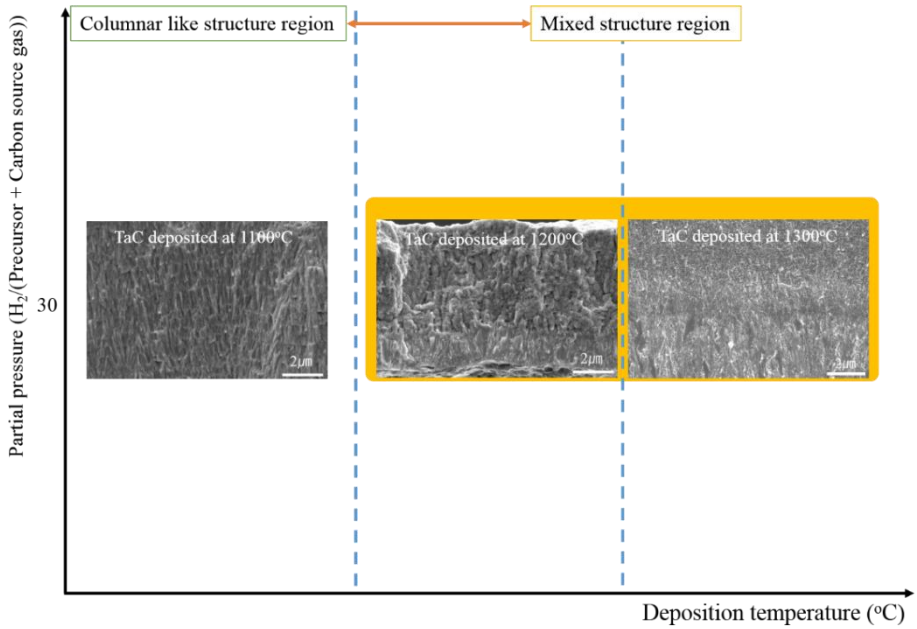

Figure 5-9. A morphological map based on the Drift model for the TaC coating layer with different deposition temperatures.

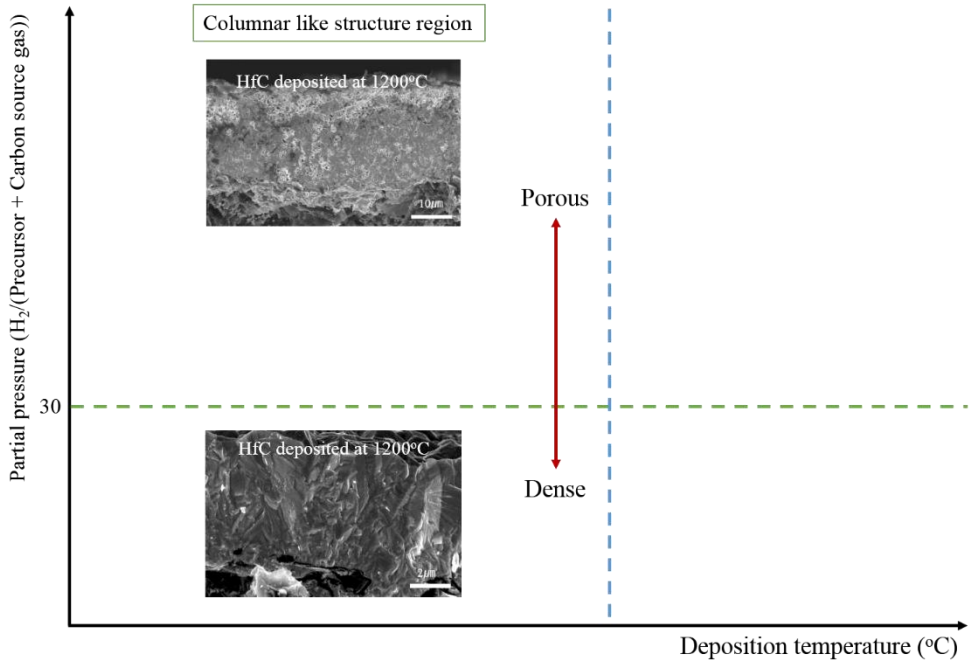

Figure 5-10. A morphological map based on the Drift model for the HfC coating layer with different deposition temperatures.

5.2 Covalent carbide

5.2.1 Silicon carbide (SiC)

Silicon carbide (SiC) was deposited on 2-inch diameter graphite substrate by chemical vapor deposition method. Deposition was carried out at different temperatures (900 – 1100 ºC). Methyltrichlorosilane (MTS : CH_3SiCl_3, KCC, Korea) was used as the source material for SiC. H_2 gas (99.999%) was utilized as the carrier and diluent gas. The input gas ratio (α: H_C+H_D/MTS) of the deposition process was set to 10.

XRD analyses of SiC layers deposited at different deposition temperatures revealed peaks corresponding to the substrate, carbon (C), and free silicon (Si) for the SiC deposited at 900°C (the lowest deposition temperature used in this study) (Figure 5-11). The presence of Si and C can result from the incomplete reaction of the SiC precursor (MTS), leading to the deposition of a thin layer. Even when deposited at the typical temperature of 1000°C, peaks related to free Si were observed, while at 1100ºC (the highest deposition temperature used in this study), peaks other than SiC were not observed.

As anticipated from the XRD results, the layer deposited at 900°C showed the presence of the substrate phase C, indicating that the deposited layer is very thin. However, microstructure observation revealed that the coating layers deposited at 900°C had a thickness of approximately 26-30 μm. Remarkably, even at such low temperatures, the typical dome-shaped microstructure commonly observed during SiC deposition was observed (Figure 5-12). As the deposition temperature increased, the deposition thickness also increased, reaching a thickness of 100 μm. SiC, being

a covalent carbide, exhibited a microstructure trend similar to that demonstrated by Chin et al. [17], rather than closely resembling the microstructure observed in SZM. At low deposition temperatures, dome-shaped microstructures were primarily observed on the surface. However, as the deposition temperature increased, faceted microstructures were reported (Figure 5-13) [16,19].

This behavior of microstructure evolution is well depicted in Figure 5-14. When compared to Chin's morphology map, where temperature acts as a significant variable, the SiC coating layer deposited at 900°C exhibited a columnar structure. However, upon changing the deposition temperature to 1100°C, a microstructure similar to the angular form observed in Chin's model was evident. Therefore, it is anticipated that increasing the deposition temperature beyond 1100°C will result in a faceted structure.

.

Table 5.3 Deposition conditions for SiC coating layers by CVD system.

Deposition temperature (°C)	Gas flow rate (sccm)			Deposition time (h)
	H_2(C)	H_2(D)	MTS	
900	73	654	73	10
1000	73	654	73	10
1100	73	654	73	10

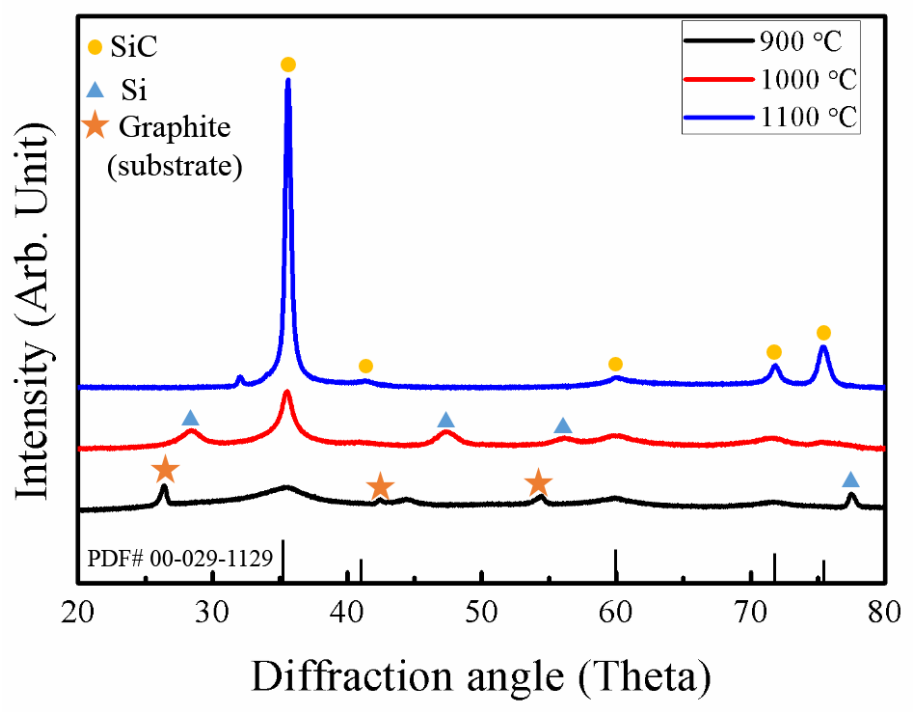

Figure 5-11. XRD results of SiC coating layers with different deposition temperatures.

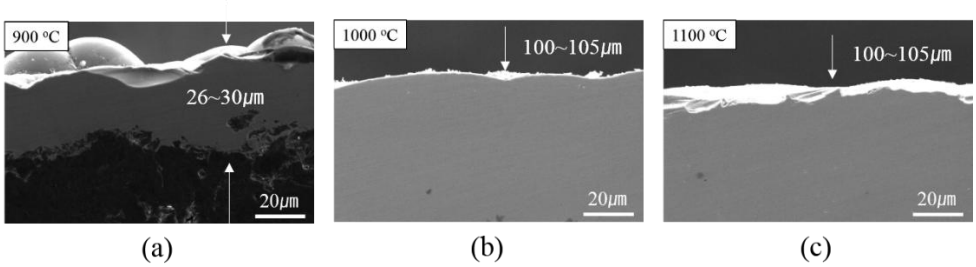

(a) (b) (c)

Figure 5-12. Cross-section Microstructure of SiC coating layers deposited at (a) 900°C, (b) 1000°C, (c) 1100°C.

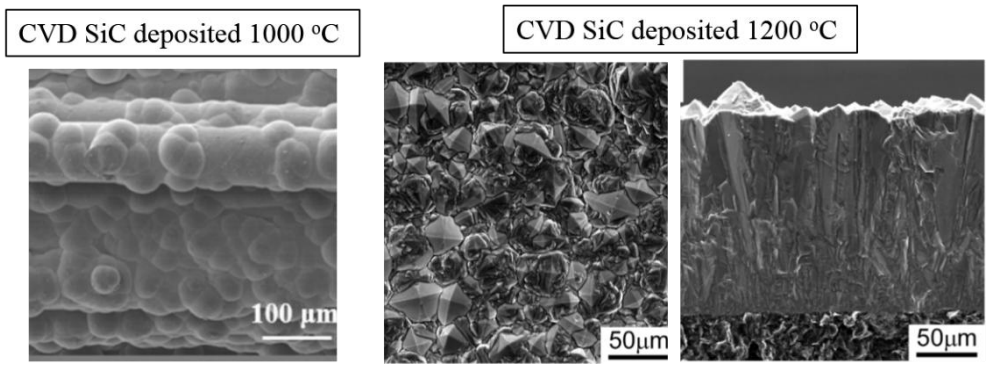

Figure 5-13. Depending on the deposition temperature of SiC, the microstructure of the surface is formed differently. In other words, the type of microstructure observed on the surface of the SiC coating layer varies with changes in the deposition temperature (Han et al, Cheng et al)[16,19]

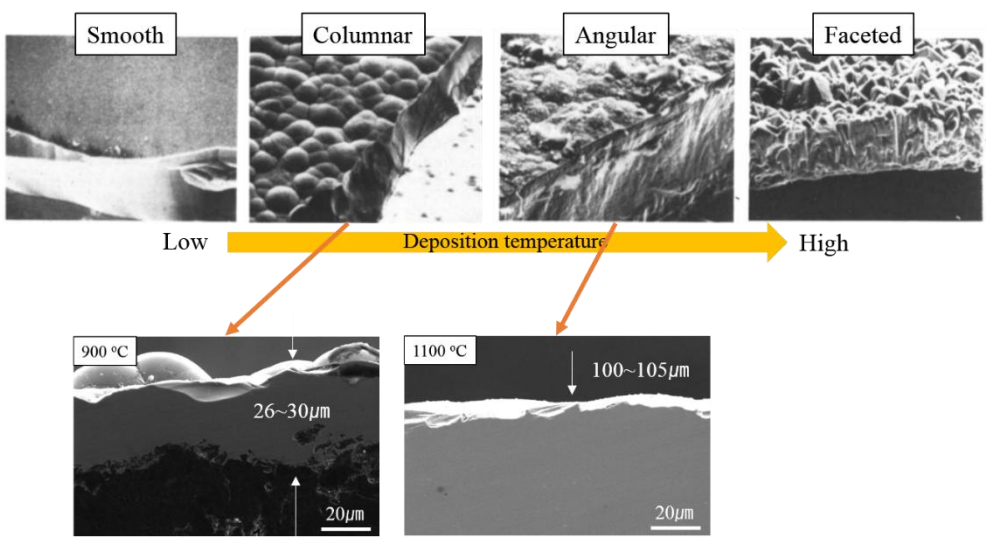

Figure 5-14. When comparing the microstructure of the as-deposited SiC coating layer with the Chin model, similarities were observed. The coating layer deposited at 900°C exhibited a columnar shape, while the one deposited at 1100°C showed an angular form [17].

5.3 References

1 H. O. Pierson, *Handbook of Chemical Vapor Deposition (CVD) Principles, Technology, and Applications*, NOYES PUBLICATIONS (1999)

2. G.B. Thompson, C.R. Weinberger, *Ultra-High Temperature Ceramics: Materials for Extreme Environment Applications*, John Wiley & Sons (2014)

3. Z.-K. Chen, X. Xiong, Y. Long, *Influence of $TaCl_5$ partial pressure on texture structure of TaC coating deposited by chemical vapor deposition*, Appl. Surf. Sci., 257 (2011) 4044–4050

4. C. Z.-Ke, X. Xiang, L. G.-Dong, S. Wei, L. Ying, *Texture structure and ablation behavior of TaC coating on carbon/carbon composites*, Appl. Surf. Sci., 257 (2010) 656–661

5. X. Xiong, Z.-K. Chen, B.-Y. Huang, G.-D. Li, F. Zheng, P. Xiao, H.-B. Zhang, *Surface morphology and preferential orientation growth of TaC crystals formed by chemical vapor deposition*, Thin Solid Films 517 (2009) 3235–3239

6. D. Kim, S. M. Jeong, S. G. Yoon, C. H. Woo, J. I. Kim, H.-G. Lee, J. Y. Park, W.-J. Kim, *Chemical Vapor Deposition of Tantalum Carbide from $TaCl_5$-C_3H_6-Ar-H_2 System*, J. Korean Ceram. Soc., 53 (2016) 597–603

7. S. Barrat, P. Pigeat, E. Bauer-Grosse, *Three-dimensional simulation of CVD diamond film growth*, Diam. Relat. Mater., 5 (1996) 276 280

8. Z. Chen, Y. Zhuo, R. Hu,W. Tu, Y. Pei, B. Fan, C. Wang, G. Wang, *Control of morphology and orientation for textured nanocrystalline indium oxide thin film: A growth zone diagram*, Mater. Des., 131 (2017) 410-418

9. L. Krishnia, P. K. Tyagi, Growth and characterization of polycrystalline diamond films on silicon using sugarcane bagasse as carbon precursor at atmospheric pressure by thermal chemical vapor deposition, Diam. Relat. Mater., 87 (2018) 18-26

10. F. Silva, F. Be´ne´dic, P. Bruno, A. Gicquel, *Formation of <110> texture during nanocrystalline diamond growth: an X-ray diffraction study*, Diam. Relat. Mater., 14 (2005) 398–403

11. M. Ohring, *Materials Science of Thin films*, Academic Press (2002)

12. Y.-L. Wang, X. Xiong, X.-J. Zhao, G.-D. Li, Z.-K. Chen, W. Sun, *Structural evolution and ablation mechanism of a hafnium carbide coating on a C/C composite in an oxyacetylene torch environment*, Corros. Sci., 61 (2012) 156–161

13. J. Ren, Y. Zhang, P. Zhang, T. Li, H. Hu, *UHTC coating reinforced by HfC nanowires against ablation for C/C composites*, Surf. Coat. Tech., 311 (2017) 191–198

14. Y.-L. Wang, X. Xiong, G.-D. Li, H.-B. Zhang, Z.-K. Chen, W. Sun, X.-J. Zhao, *Microstructure and ablation behavior of hafnium carbide coating for carbon/carbon composites*, Surf. Coat. Tech., 206 (2012) 2825–2832

15. Y ． Wang, H. Li, Q. Fu, H. Li, *Effect of deposition position on microstructure of HfC coating fabricated by low pressure chemical vapor deposition*, 18th International conference on composite materials (2011)

16. H. Cheng, R. Tu, S. Zhang, M. Han, T. Goto, L. Zhang, *Preparation of highly oriented β-SiC bulks by halide laser chemical vapor deposition*, J. Eur. Ceram. Soc.,

37 (2017) 509–515

17. J. Chin, P. K. Gantzel, R. G. Hudson, *The Structure of Chemical Vapor Deposited Silicon Carbide*, Thin Solid Films 40 (1977) 57–72

18. D. N. Lee, *Textures and related phenomena*, The National Academy of Engineering of Korea (2006)

19. X. Han, X. Chen, J. Ding, W. Wu, Z. Sun, Y. Song, *Influence of heat treatment on microstructure and mechanical properties of Cansas-II SiC/PyC/CVI-SiC mini-composites*, Ceram. Int., 48 (2022) 1077–1089

Chapter 6. Post-annealing behaviors of chemical vapor deposited ceramic carbide coatings

The post-annealing processes were applied to the high-temperature ceramic carbide (TaC, HfC, and SiC) coating layers deposited by the chemical vapor deposition (CVD) method. However, enhancement of the properties of TaC and HfC coatings through post-annealing, deposited via the CVD process at relatively low temperatures, has not been previously reported.

6.1 Interstitial carbides

6.1.1 Tantalum carbide (TaC)

In the case of the Tantalum carbide (TaC) coating layer deposited using the CVD with temperature as a variable, post-annealing resulted in a substantial improvement in crystallinity compared to the as-deposited TaC coating layers deposited at 1200°C and 1300°C (Figure 6-1). This improvement in crystallinity is a typical effect of post-annealing, leading to enhanced grain growth and structural development [1-4]. Similar phenomena have been observed in other material systems as well. Although quantitative analysis of the enhancement of crystallinity is challenging, the comparison of the intensity ratio of the main peak (111) before and after post-

annealing provides indirect verification.

Figure 6-2 illustrates the influence of post-annealing on microstructure and grain growth, as evident from the increase in XRD intensity. The microstructure underwent a transition from a mixed microstructure observed in the as-deposited state to the growth of equiaxed grain-shaped larger particles due to grain growth [5-8]. Detailed examination of the extent of grain growth revealed that the average grain size, which ranged from 800 nm to 2 μm before post-annealing, increased to size of 3-15 μm (Figure 6-3). The grain size determination was based on the EBSD results. During the post-annealing process, some pores that were not initially observed during deposition were revealed due to grain growth and atom migrations [1-4].

However, the specimens deposited at 1200ºC and 1300ºC without post-annealing and the commercial product exhibited delamination of the coating layer, leading to the exposure of the graphite substrate, as observed by the naked eye (Figure 6-4). In contrast, the specimens deposited at 1200°C and 1300°C followed by post-annealing demonstrated the integrity of the coating layer, indicating the importance of post-annealing in enhancing the structural integrity of the coating layers.

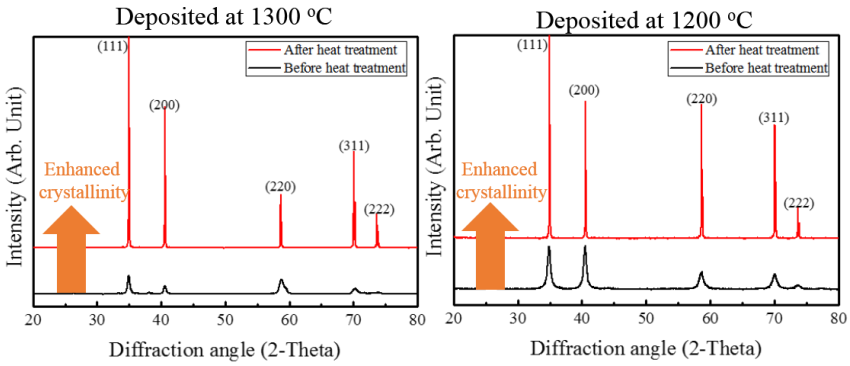

Figure 6-1. XRD results of TaC coating layers after post-annealing.

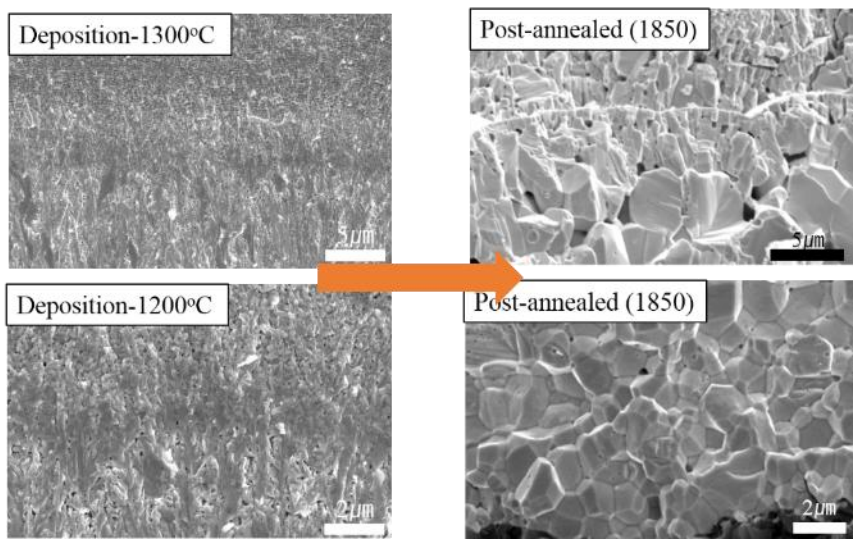

Figure 6-2. The effect of post-annealing on the microstructure of TaC coating layers deposited at 1200°C and 1300°C

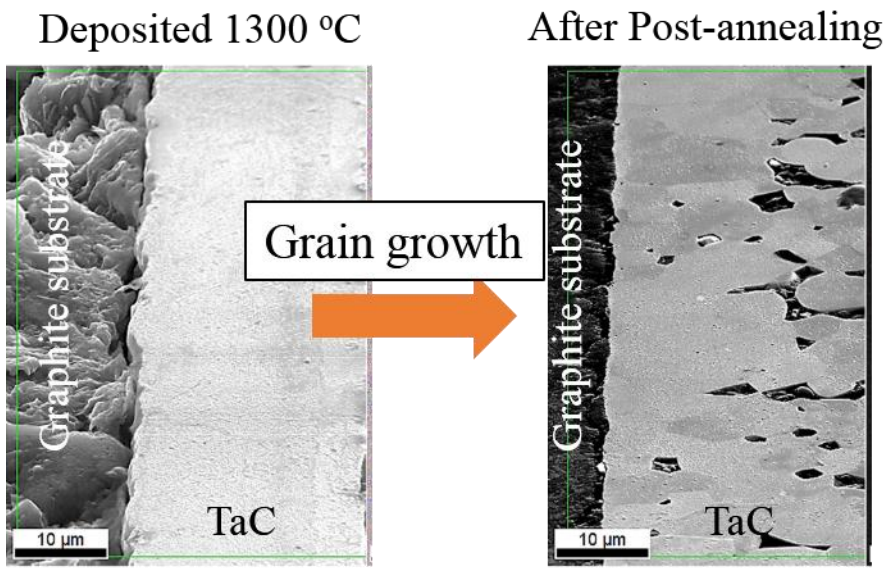

Figure 6-3. The effect of post-annealing on the grain growth of TaC coating layer deposited at 1300°C

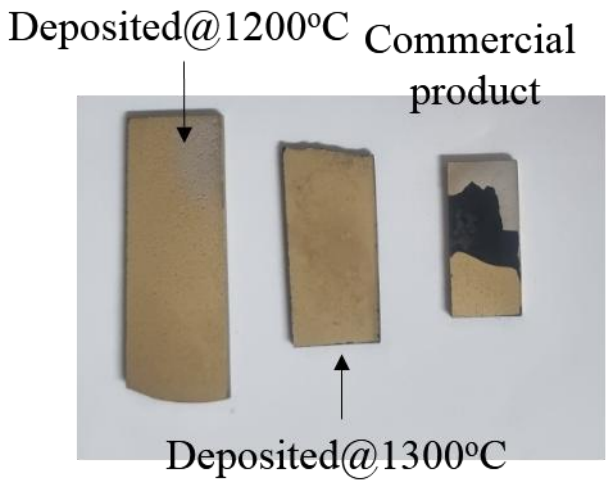

Figure 6-4. Comparing the thermal stability of specimens deposited at 1200°C and 1300°C and post-annealed commercial products, the integrity of the as-deposited coating layers was observed to be maintained.

6.1.2 Hafnium carbide (HfC)

The results of the post-annealing and XRD analysis of the Hafnium carbide (HfC) coating layer deposited using the CVD are presented in Figure 6-5. Upon post-annealing at 1600°C and 1800°C, an improvement in crystallinity was observed compared to the as-deposited coating layer. However, no additional changes, such as phase transitions or orientation shifts, were observed apart from the increase in peak intensity. This enhancement in crystallinity is consistent with the findings of Wang et al. in their study of the coating layer deposited at 1400°C [9-10]. The increase in peak intensity signifies improved ordering and structural development within the HfC coating layer.

Figure 6-6 illustrates the observed microstructure of the cross-section after post-annealing. The microstructure, which initially exhibited a mixed microstructure similar to that of as-deposited TaC, underwent a similar transformation after post-annealing. This transformation resulted in the growth of equiaxed grains within the microstructure.

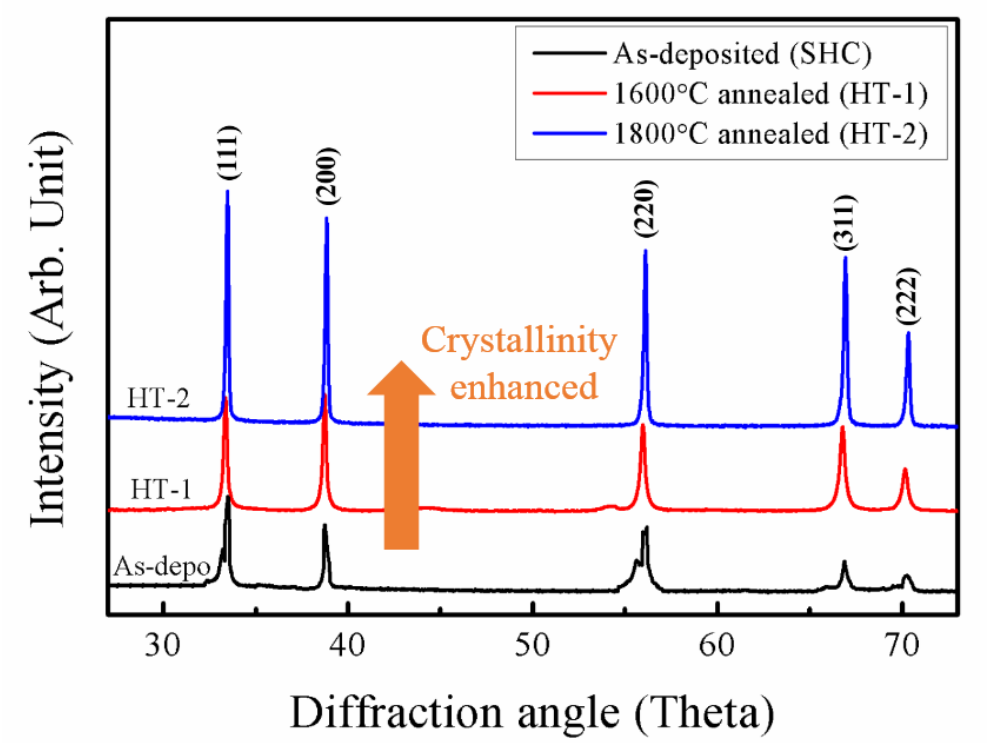

Figure 6-5. XRD results of HfC coating layers after post-annealing show that an increase in post-annealing temperature enhances the peak intensity of HfC coating layers.

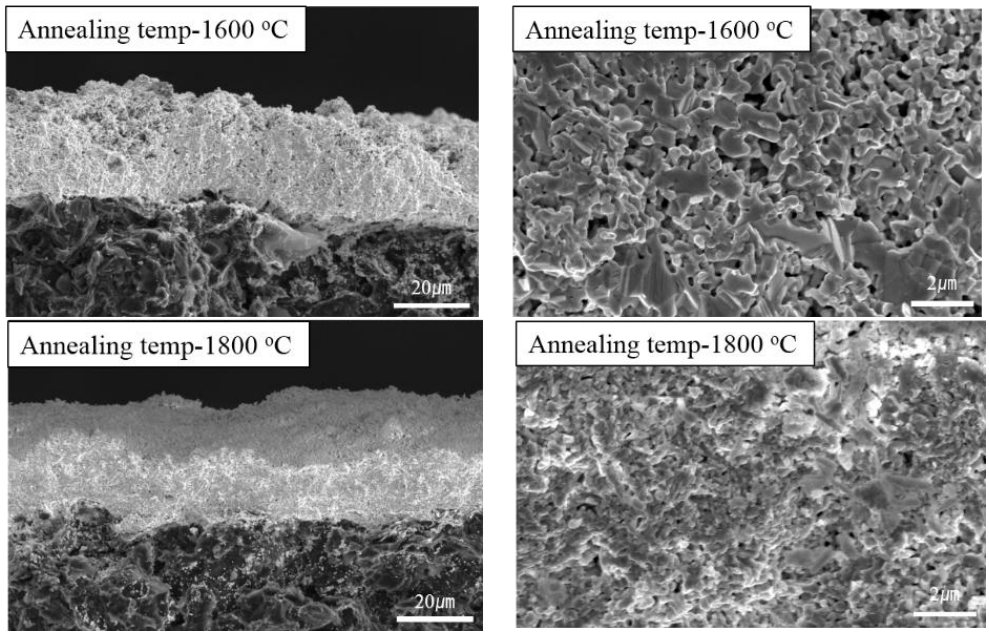

Figure 6-6. Effect of post-annealing on the microstructure of HfC coating layers: Post-annealing at 1600°C showed a fine grain structure, while post-annealing at 1800°C showed obscure grain structures by grain growth

6.1.3 Post-annealing process of TaC and HfC coating layers

Research aiming to enhance the properties of TaC and HfC coatings through post-annealing, deposited via CVD process at relatively low temperatures, has not been previously reported. Consequently, conducting direct comparisons with existing literature was challenging. However, we conducted an indirect analysis by comparing the results with those of general carbide materials or other materials subjected to post-annealing processes.

The deposition of TaC and HfC using the CVD method at lower temperatures than those typically used in manufacturing resulted in microstructures that followed the Drift model [6-8]. As discussed in the as-deposited results in Chapter 5, the microstructures at this stage exhibited columnar-like or mixed structure. A comparative analysis of the schematic and actual microstructures before and after post-annealing is presented in Figures 6-7 and 6-8. For TaC, the columnar-like structure transformed into an equiaxed microstructure after post-annealing, indicating significant microstructural evolution due to grain growth and atom migration. Similarly, the HfC coating layer exhibited a columnar-like structure, resembling TaC, but with a relatively denser microstructure. However, post-annealing revealed the presence of pores in the cross-section microstructure, attributed to the atom migration of residual pores during the process [1-4].

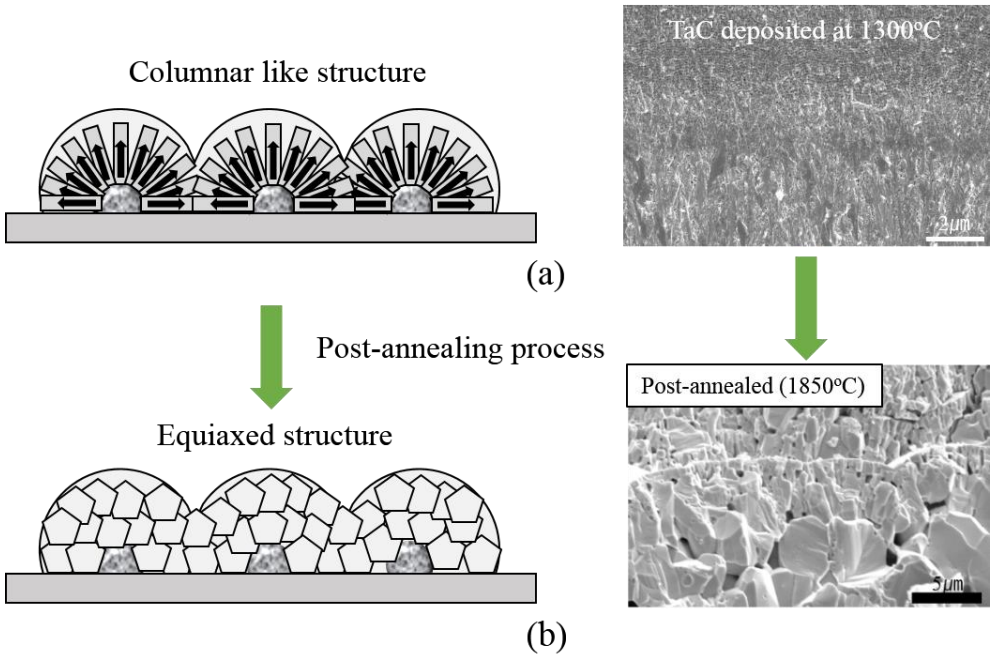

Figure 6-7. Microstructural changes on the TaC coating layer during the post-annealing. a) As-deposited TaC microstructure following the Drift model. b) Microstructural changes of TaC coating layers after the post-annealing.

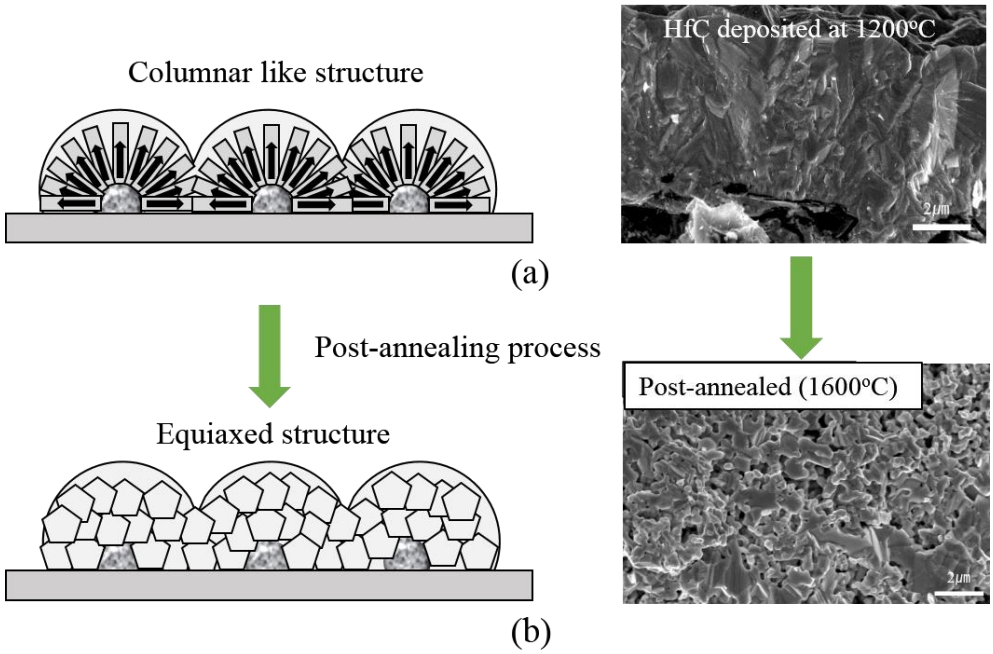

Figure 6-8. Microstructural changes on the HfC coating layer during the post-annealing. a) As-deposited HfC microstructure following the Drift model. b) Microstructural changes of HfC coating layers after the post-annealing.

6.2 Covalent carbide

6.2.1 Silicon carbide (SiC)

The X-ray diffraction (XRD) results of the post-annealed Silicon carbide (SiC) coating layer, deposited using the CVD at different temperatures, are presented in Figure 6-9. The analysis revealed that the coating layers deposited at 900°C and 1000°C exhibited improved crystallinity with increased intensity. Furthermore, the intensities of the peaks corresponding to free silicon (Si) observed in the coating layers deposited at 900°C and 1000°C were increased due to the crystallization of the free Si phase induced by post-annealing. In contrast, the XRD result of the SiC deposited at 1100°C exhibited an increased intensity only in the SiC peaks, without any other remaining phases such as Si or C.

Figure 6-10 illustrates the microstructure of the cross-sections of the SiC coating layers after post-annealing. While significant changes were not observed in the microstructure, delamination was detected in the coating layers deposited at 900°C followed by post-annealing at 1500°C. This phenomenon has been reported in various studies. For instance, Han et al. [12] demonstrated delamination in SiC composites fabricated at 1000°C and heat treated at 1500°C, which was attributed to the decomposition of the SiC matrix phase during the heat treatment. Similarly, Dong et al. [13] reported microstructural changes during a 1200°C heat treatment, leading to delamination in SiC coatings. The decrease in interfacial shear strength due to chemical instability and removal of the fiber/matrix interface during high-temperature heat treatment under vacuum was observed by Udayakumar et al. [14] and

Reynaud et al. [15] in SiC composites. Furthermore, Mei et al. [16] found that appropriate heat treatment at 1200°C improved the mechanical properties of SiC coatings by eliminating residual thermal stresses between the matrix and fibers generated during the deposition/infiltration process.

The problem of delamination in SiC coatings can be attributed to the grain growth induced by high post-annealing temperatures, which causes shrinkage of boundaries or grooves within the coating layer and compromises its structural integrity [15-16]. This phenomenon is exemplified in Figure 6-11, where the delamination is observed in the matrix and coating layer of SiC fiber-reinforced composites after heat treatment at 1500°C [12]. The likelihood of such delamination is higher in the temperature region near the decomposition of the fibers.

Additionally, even at heat treatment temperature of 1200°C (Figure 6-12) [13], delamination was observed in SiC coated layers. To achieve the desired crystallinity and microstructure in the deposited SiC coating layer, conducting a post-annealing process at 1200°C is deemed most suitable. At this temperature, it is possible to attain improved crystallinity without promoting excessive grain growth and the associated delamination.

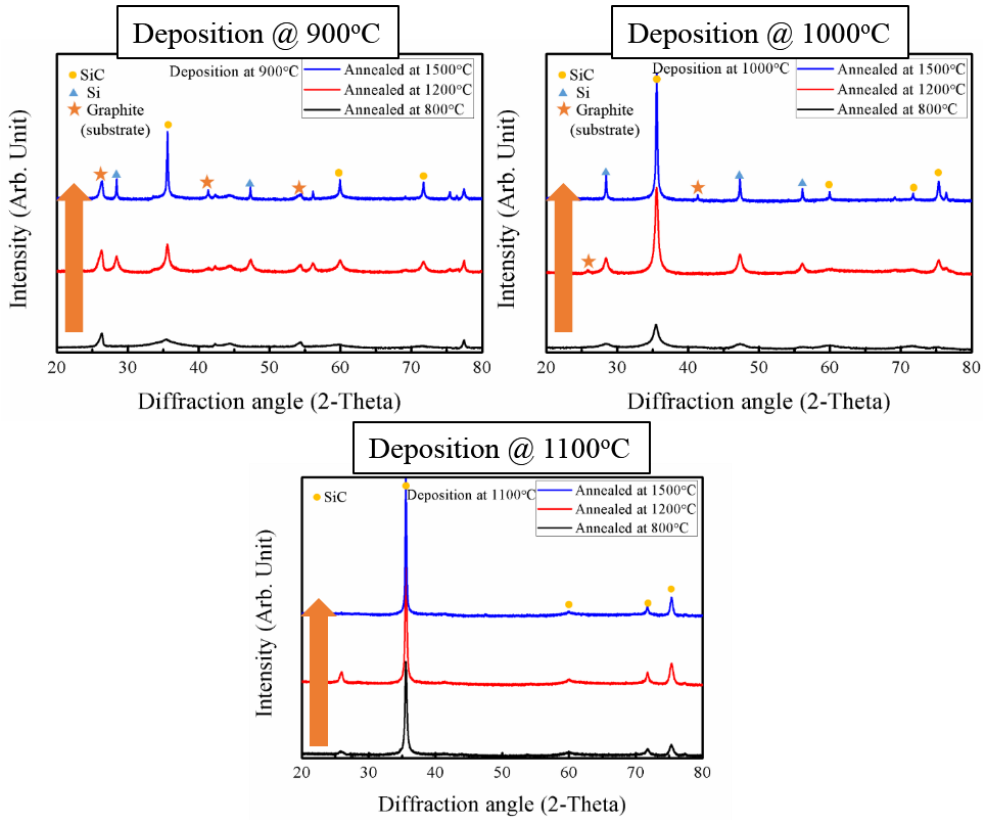

Figure 6-9. XRD results of the SiC coating layer after the post-annealing: The coating layers deposited at 900°C and 1000°C showed increased Si and SiC peaks. At 1100°C, only the SiC peak was observed with enhanced crystallinity.

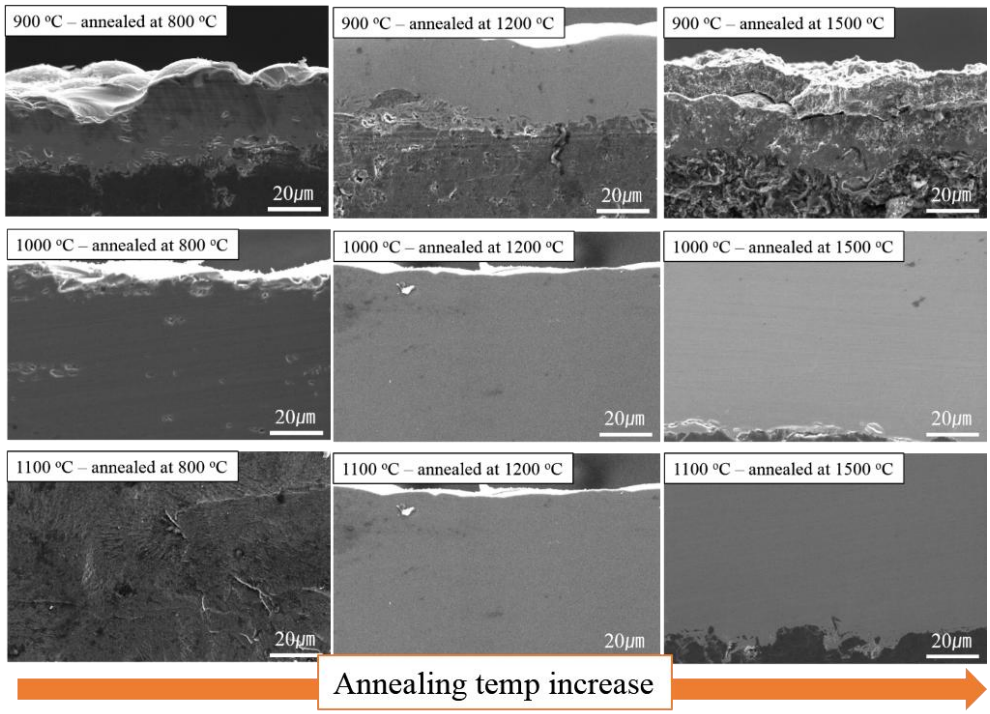

Figure 6-10. Effect of post-annealing on the microstructure of the SiC coating layer: Increasing the annealing temperature shows no significant changes in the cross-sectional microstructures. Only the coating layers deposited at 900°C and annealed at 1500°C exhibit delamination.

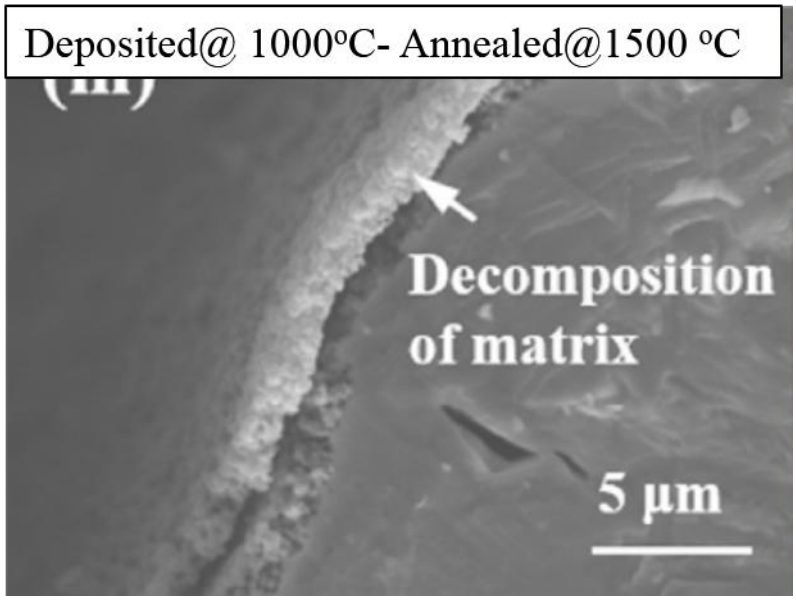

Figure 6-11. Decomposition of SiC Matrix/SiC coating layer (Han et al)[12]

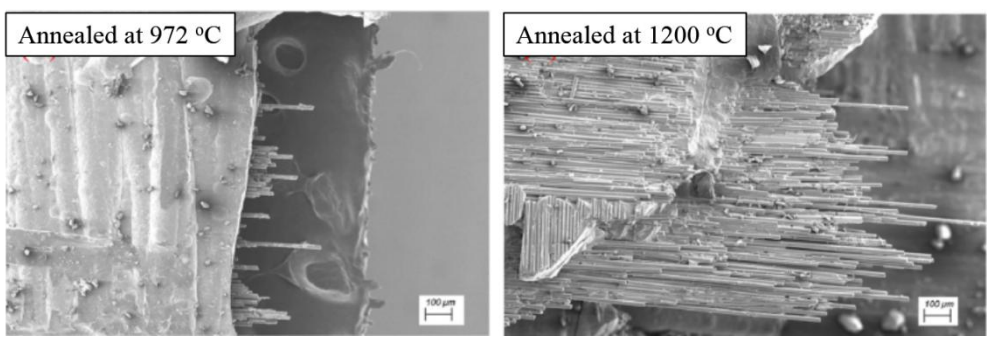

Figure 6-12. After post-annealing, the SiC composite fabricated at 972°C shows no significant change. However, the composites fabricated at 1200°C showed delamination in their microstructure during post-annealing (Dong et al)[13]

6.3 References

1. E. Colombini, M. Lassinantti Gualtieri, R. Rosa, F. Tarterini, M. Zadra, A. Casagrande, P. Veronesi, *SPS-assisted Synthesis of SICp reinforced high entropy alloys: reactivity of SIC and effects of pre-mechanical alloying and post-annealing treatment*, Powder Metall., 61 (2018) 64-72

2. F. Zhang, S. Yan, C. Li, Y. Ding, J. He, F. Yin, *Synthesis and characterization of MAX phase Cr_2AlC based composite coatings by plasma spraying and post annealing*, J. Eur. Ceram. Soc., 39 (2019) 5132–5139

3. B. Suleiman, H. Zhang, Y. Ding, Y. Li, *Microstructure and mechanical properties of cold sintered porous alumina ceramics*, Ceram. Int., 48 (2022) 13531–13540

4. L. Zhao, F. Zhang, L. Wang, Shu Yan, J. He, F. Yin, *Effects of post-annealing on microstructure and mechanical properties of plasma sprayed Ti-Si-C composite coatings with Al addition*, Surf. Coat. Tech., 416 (2021) 127164

5. M. Ohring, *Materials Science of Thin films*, Academic Press (2002)

6. Z. Chen, Y. Zhuo, R. Hu,W. Tu, Y. Pei, B. Fan, C. Wang, G. Wang, *Control of morphology and orientation for textured nanocrystalline indium oxide thin film: A growth zone diagram*, Mater. Des., 131 (2017) 410-418

7. L. Krishnia, P. K. Tyagi, Growth and characterization of polycrystalline diamond films on silicon using sugarcane bagasse as carbon precursor at atmospheric pressure by thermal chemical vapor deposition, Diam. Relat. Mater., 87 (2018) 18-26

8. F. Silva, F. Be´ne´dic, P. Bruno, A. Gicquel, *Formation of <110> texture during nanocrystalline diamond growth: an X-ray diffraction study*, Diam. Relat. Mater., 14 (2005) 398–403

9. Y.-L. Wang, X. Xiong, G.-D. Li, H.-B. Zhang, Z.-K. Chen, W. Sun, X.-J. Zhao, *Microstructure and ablation behavior of hafnium carbide coating for carbon/carbon composites*, Surf. Coat. Tech., 206 (2012) 2825–2832

10. Y.-L. Wang, X. Xiong, X.-J. Zhao, G.-D. Li, Z.-K. Chen, W. Sun, *Structural evolution and ablation mechanism of a hafnium carbide coating on a C/C composite in an oxyacetylene torch environment*, Corros. Sci., 61 (2012) 156–161

11. J. Chin, P. K. Gantzel, R. G. Hudson, *The Structure of Chemical Vapor Deposited Silicon Carbide*, Thin Solid Films 40 (1977) 57–72

12. X. Han, X. Chen, J. Ding, W. Wu, Z. Sun, Y. Song, *Influence of heat treatment on microstructure and mechanical properties of Cansas-II SiC/PyC/CVI-SiC mini-composites*, Ceram. Int., 48 (2022) 1077–1089

13. H. Dong, X. Gao, S. Zhang, Y. Song, J. Yang, Fang Wang, *Effects of heat treatment on the mechanical properties at elevated temperatures of plain-woven SiC/SiC composites*, J. Eur. Ceram. Soc., 42 (2022) 412–419

14. A. Udayakumar, A.S. Ganesh, S. Raja, M. Balasubramanian, *Effect of intermediate heat treatment on mechanical properties of SiCf/SiC composites with BN interphase prepared by ICVI*, J. Eur. Ceram. Soc., 31 (6) (2011) 1145–1153

15. P. Reynaud, D. Rouby, G. Fantozzi, *Effects of temperature and of oxidation on the interfacial smear stress between fibres and matrix in ceramic-matrix composites*, Acta Mater., 46 (7) (1998) 2461–2469.

16. H. Mei, H. Zhang, W.Z. Huang, M. Han, Y.W. Xu, L.F. Cheng, *Effects of heat treatment temperatures on microstructures and mechanical properties of the chopped carbon fibres SiC composites*, Adv. Appl. Ceram., 117 (7) (2018) 389–394

Chapter 7. Effect of post-annealing on the nano hardness of carbide coating layers

The nano hardness of the deposited coating layer was measured both in the as-deposited state and after post-annealing to assess changes in mechanical properties. Notably, interstitial carbides exhibited significant changes microstructure changes and crystallinity improvement after post-annealing, indicating a considerable impact on their mechanical properties compared to covalent carbides.

7.1 Interstitial carbide

7.1.1 Tantalum carbide (TaC)

TaC in the as-deposited state exhibits the highest hardness value of 28 GPa when deposited at 1100ºC (Figure 7-1). This is due to twinning caused by a columnar microstructure with (111) orientation[1-2]. However, as the deposition temperature is increased, the hardness value is gradually decreased. This can be attributed to the transformation of the microstructure from columnar to a structure following the Van der Drift model[2], resulting in a reduction of twin planes and relatively less occurrence of internal strain deformation. As shown in Figure 5-2, TaC deposited at 1100°C exhibits a columnar structure. However, as the deposition temperature is increased, the columnar structure disappears and transforms into a ball-like structure suggested by the Van der Drift model, which influences the decrease in nano

hardness. Nevertheless, it is noteworthy that the TaC coating layer deposited at 1300°C shows a higher hardness value compared to commercially produced TaC prepared at high temperatures; near 2000°C[3-4]. Furthermore, when compared to a coating layer consisting of a mixture of TaC and Ta_2C, this mixed phase coating layer exhibits low hardness values due to the brittle nature of Ta_2C (average hardness: 10-12 GPa).

Figure 7-2 represents the measured nano hardness values of the CVD TaC coating layer after post-annealing. After post-annealing, an approximate 10% increase in hardness was observed for both commercially produced TaC and coating layers deposited at 1200°C and 1300°C. This improvement in hardness can be attributed to the transformation of the mixed microstructures into equiaxed structures and the enhancement of crystallinity during the post-annealing. Additionally, the improvement in commercial TaC can be attributed to the alleviation of thermal stress that was originally present within the coating layer due to high-temperature deposition, which was resolved through post-annealing and other processes. In comparison to other research findings, it was difficult to make quantitative comparisons as there have been no previous results of post-annealing processes conducted on TaC coating layers deposited using the CVD method at low temperatures. Therefore, resorting to comparing with commercially available samples was the only feasible approach.

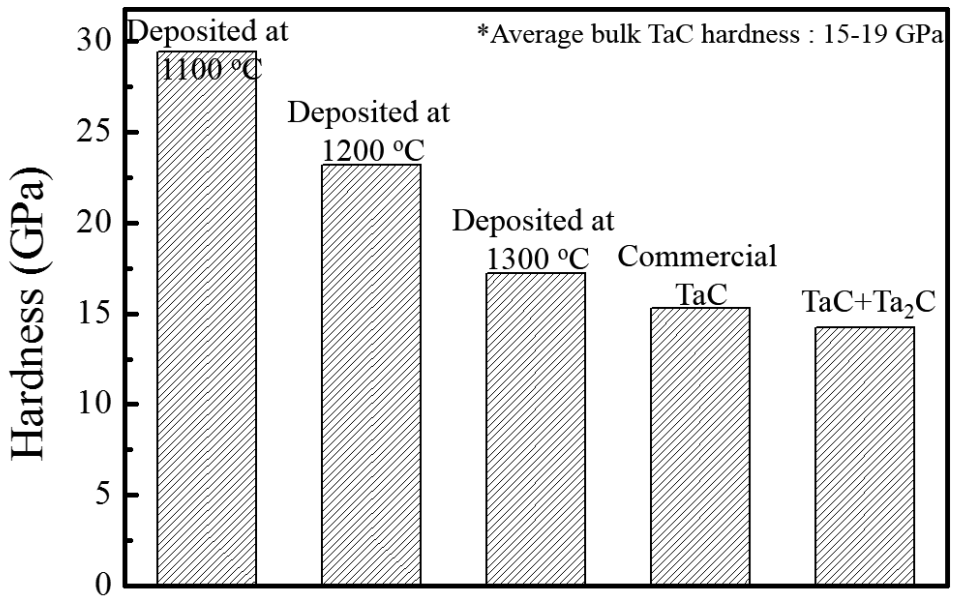

Figure 7-1. Nano hardness of as-deposited CVD TaC coating layers: Lowering the deposition temperature results in a decrease in hardness value. The TaC coating layer deposited at 1300°C has a higher hardness value than the commercial product.

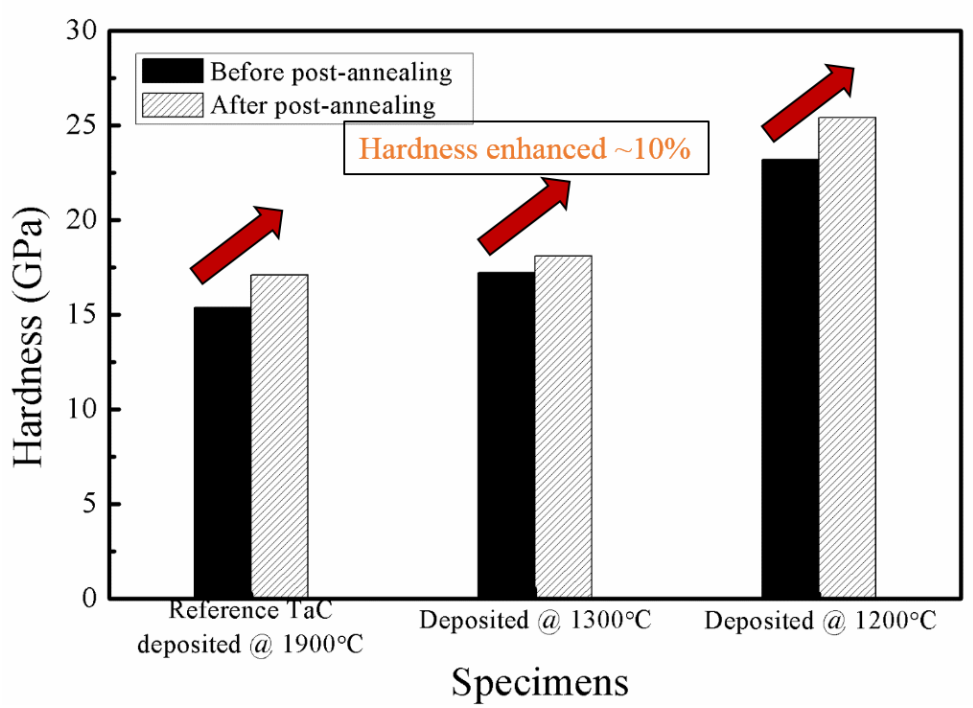

Figure 7-2. Nano hardness of CVD TaC coating layers showed changes by post-annealing.

7.1.2 Hafnium carbide (HfC)

The as-deposited CVD HfC coating layer exhibited a low hardness value despite the high intensity of XRD results which showed high crystallinity and a single phase. This can be attributed to the presence of a mixed microstructure rather than a complete columnar structure due to the low-temperature deposition process, resulting in a lack of twin plane structures and consequently lower nano hardness values. However, it was observed that the hardness value was gradually improved when the crystallinity was enhanced and the microstructure was controlled to an equiaxed form through post-annealing. This can be attributed to grain growth and microstructural evolution occurring during the post-annealing[5]. Furthermore, when compared to the hardness values of coating layers with excess carbon, it was evident that the influence of carbon, which tends to have a relatively softer nature, resulted in significantly lower hardness values. Through the post-annealing process, the hardness value of the HfC coating layer produced at 1200°C was enhanced to a level similar to that of HfC coating layers known to be produced at high temperatures[3-4].

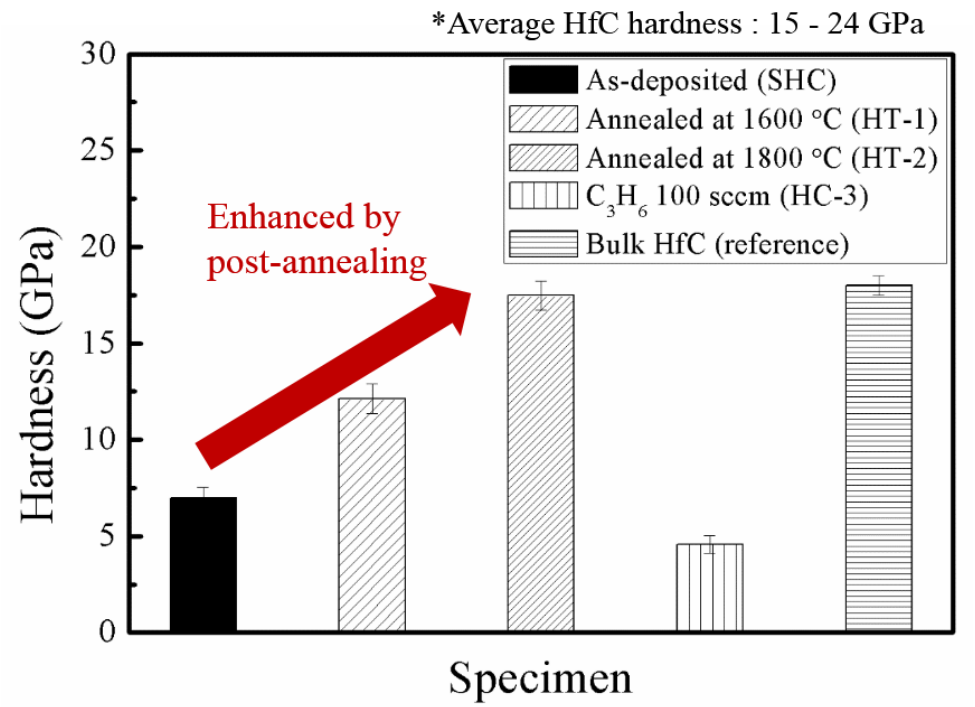

Figure 7-3. Nano hardness of CVD HfC before and after post-annealing: The as-deposited HfC coating layer showed a very low hardness compared to the reported value (Thompson et al)[3-4]. After post-annealing, the hardness value is improved due to enhancement of crystallinity.

7.2 Covalent carbide

7.2.1 Silicon carbide (SiC)

The nano hardness values of SiC coating layers deposited by CVD at different temperatures are presented in Figure 7-4. SiC deposited at 900ºC showed an average hardness value of 19.93 GPa, which is lower than the average hardness of SiC films (37-42GPa)[3-4]. As the deposition temperature was increased, the nano hardness was increased up to 27.75 GPa. This can be attributed to the improved crystallinity with increasing deposition temperature[6-8]. Guicciardi et al.[9] compared the hardness of SiC based on the particle size. It was observed that SiC with small particle size exhibited a high hardness value of 35 GPa. However, the measured average hardness ranged from 30-35 GPa. To enable a more precise comparison, the researchers also examined the nano hardness of irradiated SiC composites that were subjected to a treatment akin to heat treatment. In this instance, a declining trend was observed in comparison to the hardness values measured at room temperature, which ranged from 38-40 GPa[10].

Figure 7-5 illustrates the change in nano hardness of SiC coating layers when subjected to post-annealing at various temperatures. When post-annealing was performed at 800°C and 1200°C, the nano hardness exhibited an increasing trend compared to the as-deposited state. However, when post-annealing was conducted at 1500°C, a decreasing trend in nano hardness was observed. Particularly, the coating layer deposited at 1100°C and post-annealed at 1500°C showed a significant

decrease in nano hardness. The cause of these changes can be understood from the observed surface microstructure in Figure 7-6. Numerous cracks were observed in the surface region after heat treatment at 1500°C, and the presence of these cracks internally led to a degradation in nano hardness. These cracks can be attributed to the reduction in surface energy caused by grain growth during the post-annealing process[11].

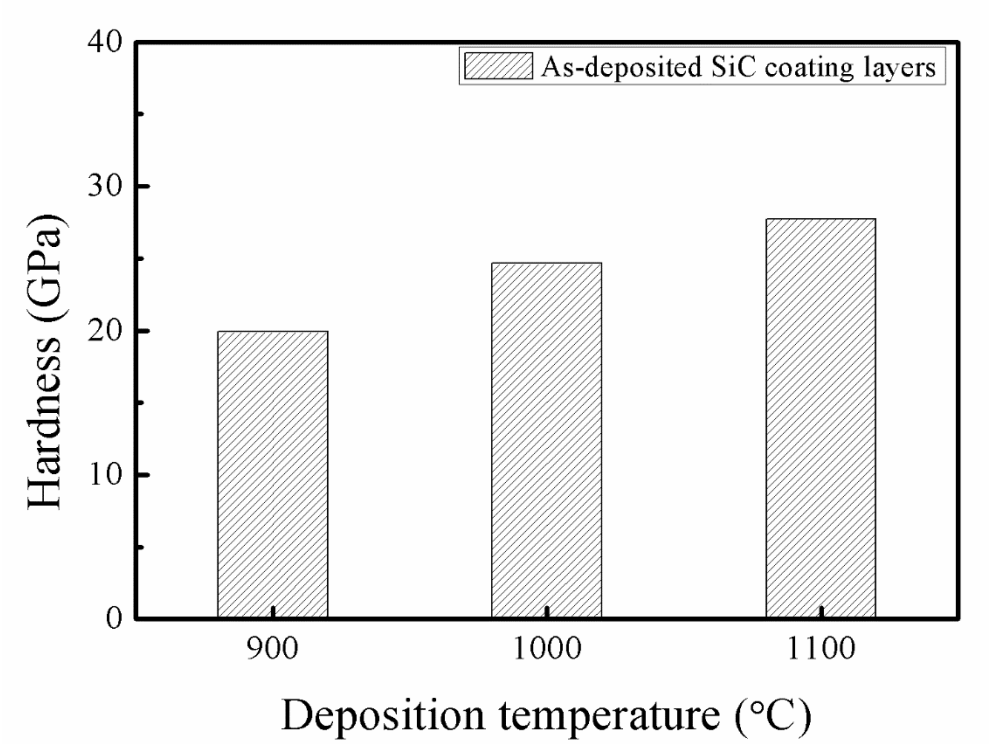

Figure 7-4. Nano hardness of as-deposited CVD SiC coating layers: The hardness value increases as the deposition temperature changes due to the high crystallinity of the deposited coating layer.

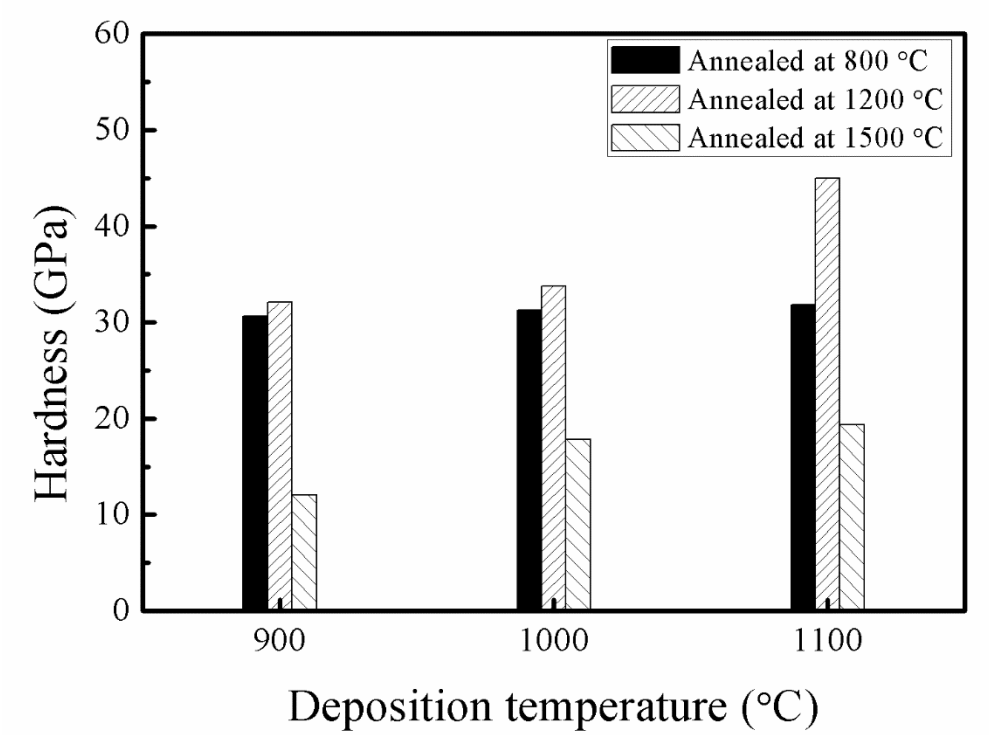

Figure 7-5. Nano hardness of CVD SiC coating layers showed changes after post-annealing. Post-annealing at 800°C and 1200°C resulted in increased hardness values. However, coating layers annealed at 1500°C exhibited a significant decrease in hardness value due to delamination.

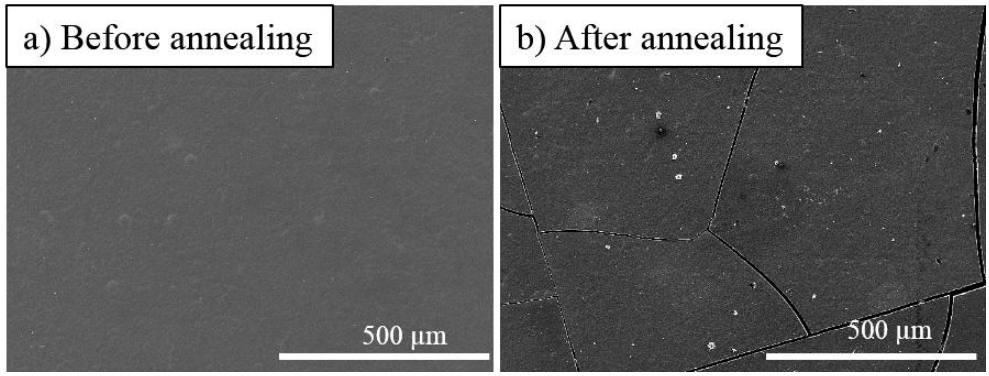

Figure 7-6. The surface microstructure of SiC deposited at 900°C before and after post-annealing at 1500°C. a) The surface showed a smooth structure. b) Cracks were observed on the surface.

7.3 References

1. X. Xiong, Z.-K. Chen, B.-Y. Huang, G.-D. Li, F. Zheng, P. Xiao, H.-B. Zhang, *Surface morphology and preferential orientation growth of TaC crystals formed by chemical vapor deposition*, Thin Solid Films 517 (2009) 3235–3239

2 F. Silva, F. Be´ne´dic, P. Bruno, A. Gicquel, *Formation of <110> texture during nanocrystalline diamond growth: an X-ray diffraction study*, Diam. Relat. Mater., 14 (2005) 398–403

3. H. O. Pierson, *Handbook of Chemical Vapor Deposition (CVD) Principles, Technology, and Applications*, NOYES PUBLICATIONS (1999)

4. G.B. Thompson, C.R. Weinberger, *Ultra-High Temperature Ceramics: Materials for Extreme Environment Applications*, John Wiley & Sons (2014)

5. R. Hu, J. Zhang, R. Wang, C. Zhang, Z. Xie, Y. Zhang, G. Li, X. Lu, *Effect of heat treatment on microstructure and properties of WC reinforced co-based composite coating on copper*, Mater. Lett., 319 (2022) 132262

6. H. Dong, X. Gao, S. Zhang, Y. Song, J. Yang, Fang Wang, *Effects of heat treatment on the mechanical properties at elevated temperatures of plain-woven SiC/SiC composites*, J. Eur. Ceram. Soc., 42 (2022) 412–419

7. X. Han, X. Chen, J. Ding, W. Wu, Z. Sun, Y. Song, *Influence of heat treatment on microstructure and mechanical properties of Cansas-II SiC/PyC/CVI-SiC mini-composites*, Ceram. Int., 48 (2022) 1077–1089

8. H. Mei, H. Zhang, W. Huang, M. Han, Y. Xu, L. Cheng, *Effects of heat treatment temperatures on microstructures and mechanical properties of the chopped carbon fibres SiC composites*, Adv. Appl. Ceram., 117 [7] (2018) 389–394

9. S. Guicciardi, A. Balbo, D. Sciti, C. Melandri, G. Pezzotti, *Nanoindentation characterization of SiC-based ceramics*, J. Eur. Ceram. Soc., 27 (2007) 1399–1404

10. D. Frazer, C.P. Deck, P. Hosemann, *High-Temperature Nanoindentation of SiC/SiC Composites*, JOM-J. Min. Met. Mat. S., 72 (2020) 139-144.

11. D. N. Lee, Textures and related phenomena, The National Academy of Engineering of Korea (2006)

Chapter 8. Summary

The effect of post-annealing on the crystallinity, microstructure and mechanical properties of refractory transition metal carbide (TaC, HfC, SiC) coating layers deposited by chemical vapor deposition (CVD) at low temperature was investigated.

It was difficult to find prior results on the effect of post-annealing on the crystallinity, microstructure, and mechanical properties of carbide coating layers deposited at low temperature. Most CVD coating layers are primarily deposited at high temperatures to achieve high crystallinity and mechanical properties. However, fabricating at high temperatures has drawbacks, including damaging the fibers when producing fiber-reinforced composites and the inability to control the microstructure. Therefore, unlike previous studies, the aim of this work was to deposit the coating layers at relatively low temperatures, which can result in decreased crystallinity and compromised mechanical properties. To address these limitations, we implemented a post-annealing process to enhance crystallinity and control the microstructure, ultimately achieving levels of nano hardness and coating layer integrity which are comparable to those obtained with coating layers deposited at high-temperature.

Specifically, we applied the post-annealing process to the TaC and HfC coating layers deposited at different temperatures and to the SiC coating layers deposited at varying precursor pressures. TaC and HfC are categorized as interstitial carbides with higher melting points and have superior high-temperature characteristics compared to SiC, which is classified as a covalent carbide. Moreover, the deposition

mechanism and microstructural changes following post-annealing exhibited distinct behaviors for TaC, HfC, and SiC. SiC demonstrated a columnar structure in cross-section, as per Chin's proposed CVD SiC morphology map, while the surface microstructure varied with deposition temperature. On the other hand, TaC and HfC were analyzed using the existing structural zone model and Van der Drift's model since a morphology map specific to them was not available. Both models indicated an initial growth behavior resembling columnar or similar structures. However, it was observed that the shape and grain size of the microstructure were influenced by temperature and precursor pressure.

1. When deposited at low temperatures, TaC and HfC exhibited comparable growth structures resembling columnar structures. However, after undergoing post-annealing, this initially similar microstructure transformed into equiaxed structures due to grain growth. Consequently, this transformation led to an approximate 10% increase in crystallinity and nano hardness.

2. SiC, as a covalent carbide, exhibited surface morphology consistent with the existing models. Post-annealing contributed to improved crystallinity; however, at 1500°C, excessive grain growth, cracks, and delamination were observed on the surface.

Hence, the key finding of this study is that by considering the microstructure growth mechanism based on the specific material when depositing ceramic carbide coating layers at low temperatures and applying a post-annealing process, it is

possible to achieve properties similar to those attained through high-temperature manufacturing.

Publications

1. D. Kim*, J. Han, C. Park, H.-G. Lee, J.Y. Park, W.-J. Kim, *Chemical Vapor Deposition of Dense Hafnium Carbide from $HfCl_4$-C_3H_6-H_2 system for the Protection of Carbon Fibers*, Advanced Engineering Materials (2018)

2. J. Han, D. Kim, H.-G. Lee, W.-J. Kim, C. Park, J.Y. Park*, *Influence of crystallinity on the corrosion rate of chemically vapor-infiltrated SiC_f/SiC composites under 310°C hydrothermal condition*, International Journal of Applied Ceramic Technology (2021)

3. J. Han, D. Kim, S.-Y. Lee, W.-J. Kim, C. Park, J.Y. Park*, *Influence of CVI process time on the C-ring strength of hybrid SiC_f/SiC composites fabricated by CVI-LSI*, Journal of the Korean Ceramic Society (2022)

4. J. Han, S.M. Jeong, J.Y. Park, H.-G. Lee, W.-J. Kim, C. Park, D. Kim*, *Microstructural evolution of chemically vapor-deposited tantalum carbide at elevated temperature*, Journal of Ceramic Processing Research (2022)

국문 초록

후열처리가 저온 화학기상증착법으로 증착한 탄화물계 세라믹스(TaC, HfC, SiC)의 미세구조와 특성에 미치는 영향

한장원

공과대학 재료공학부

서울대학교

후열처리가 저온 화학기상증착법(CVD)으로 증착한 탄화물(TaC, HfC, SiC)의 미세구조와 특성에 미치는 영향을 조사하기 위해, 탄화물 코팅층을 CVD법을 사용하여 흑연 기판에 증착한 후 다양한 조건에서 후 열처리를 진행하였고, 증착-후열처리 조건과 미세구조-기계적 특성 간의 관계를 연구하였다.

탄탈륨 카바이드(TaC) 코팅층은 $TaCl_5$-C_3H_6-H_2 CVD 시스템을 사용하여 다양한 증착 조건아래 흑연 기판 위에 증착하였다. 증착된 TaC 코팅층은 결정학적 우선 방향성을 가지며, (111) 및 (200) 방향이 우세한 것으로 나타났다. 하지만, 증착 온도가 증가함에 따라 우선 방향이 무작위 방향성으로 변화하였다. 증착된 코팅층에 시행된 후 열처리공정은 코팅층의 결정성을 크게 향상시켰다. 증착온도를 1100℃부터 1300℃로 변화시키면서 증착하는 경우, 미세구조는 주상정형태의 구조와 주상정-등축 혼합 구조를 보였다. 코팅층에 행해진 후 열처리 공정은 입자 성장을 유발하여 미세구조가 주상정에서 등축형으로 변화하게 만들었다. 이

러한 결과는 후 열처리가 저온에서 증착한 TaC 코팅층의 결정성을 향상시키고, 기계적 물성을 10%가량 증가시킬 수 있는 변화를 보여주고 있다.

하프늄 카바이드(HfC) 코팅층은 $HfCl_4$–C_3H_6–H_2 CVD 시스템을 사용하여 1200℃에서 흑연 기판에 증착하였다. 증착된 코팅층은 높은 결정성과 조밀한 미세구조(주상정 형태)를 보였다. 증착된 코팅층에 시행된 후 열처리 공정은 코팅층의 미세구조에 영향을 미쳐 주상정형태를 등축상 형태로 변화시키고, 기공구조가 드러나게 만들었다. 코팅층의 나노 경도도 후 열처리 과정에서 향상되었다. 이러한 결과는 1200℃에서 증착된 HfC 코팅층이 조밀한 미세구조를 가지고 있으며, 그 결정성과 나노 경도가 후 열처리를 통해 향상될 수 있다는 것을 보여주고 있다.

실리콘 카바이드(SiC) 코팅층은 다양한 증착 온도에서 CVD 방법을 사용하여 흑연 기판에 증착하였다. X선 회절(XRD) 분석 결과 증착 온도에 따라 코팅층의 결정성이 변화함을 보였다. 900℃에서 증착된 코팅층에서는 유리 실리콘(free Si)의 피크가 관찰되었지만, 전구체의 완전한 반응으로 인해 높은 증착 온도에서는 증착된 코팅층에서 실리콘 피크가 관찰되지 않았다. 높은 증착 온도에서 증착된 코팅층의 두께가 증가하는 경향을 보였다. 후 열처리는 증착된 코팅층의 결정성을 향상시켰다. 코팅층의 나노 경도도 또한 온도에 따라 변화하였다. 이러한 결과는 후 열처리가 SiC 코팅층의 결정성, 미세구조 및 나노 경도를 향상시킬 수 있다는 것을 보여준다.

TaC, HfC, SiC는 탄화물 기반의 코팅층이지만, 그들의 미세구조의 성장 메커니즘은 유사하면서도 약간 다르다. 따라서, 후 열처리 과정에서 발생하는 미세구조의 변화도 다양하다. 특히, TaC, HfC와 SiC는 후 열처리 후에 부분적으로 차이를 보이며, 그 차이를 본 논문에서 간략히 논의

하였다.

본 연구는 고온 세라믹 탄화물(TaC, HfC, SiC)의 결정성, 미세구조 및 후 열처리가 미세구조-기계적 특성에 미치는 영향을 조사함으로써 높은 온도에서 나타나는 이러한 세라믹 탄화물의 우수한 특성에 대한 포괄적이고 상세한 연구의 방향성을 제공한다. 이러한 연구 결과는 고온 세라믹 탄화물의 우수한 특성에 대한 이해를 높이는 데 기여할 수 있을 것으로 보인다.

Appendix

1.Tantalum carbide deposition with different deposition positions

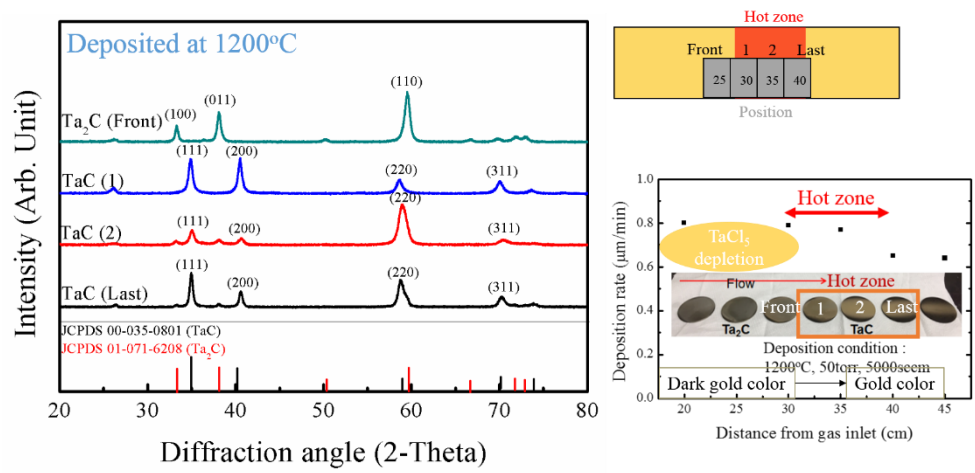

Figure 1. TaC coating layer deposited at 1200°C with different deposition positions. Due to variations in the flow rate depending on the deposition location, the intensity of the TaC phase was observed to differ. Additionally, this led to different colorations being observed in the deposited coating layer.

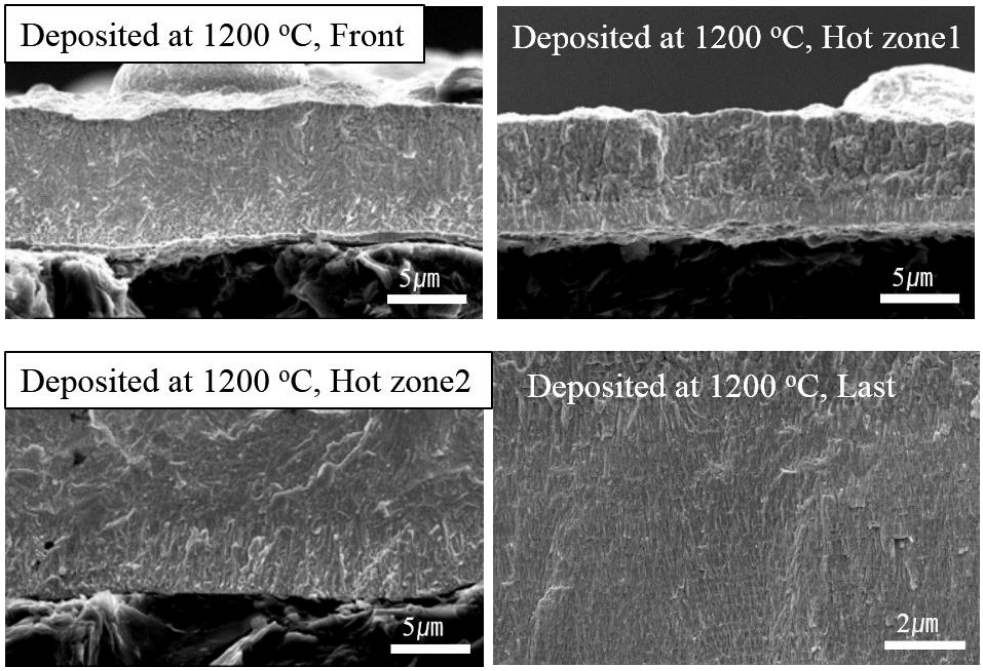

Figure 2. Microstructural observation of TaC coating layer deposited at 1200ºC with different deposition positions.

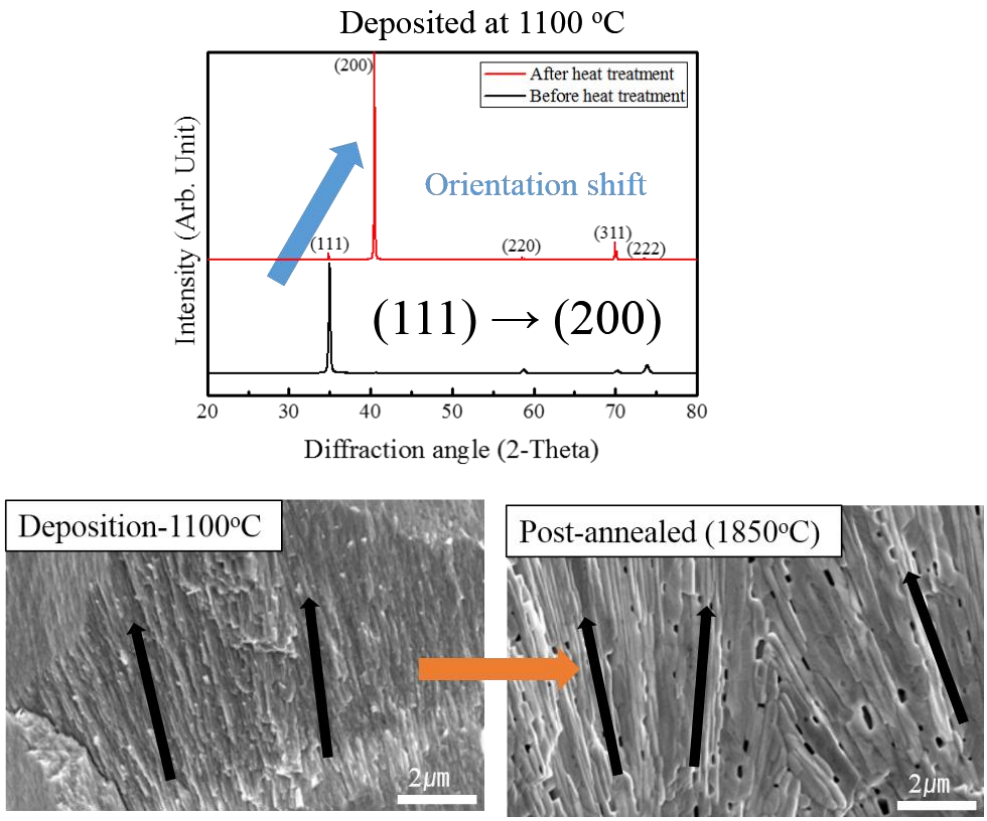

Figure 3. The XRD and microstructural changes of the TaC coating deposited at 1100°C after post-annealing were observed. In the XRD analysis, the orientation shifted from the (111) peak to the (200) peak, but no changes were observed in the microstructure, revealing only the presence of pores.

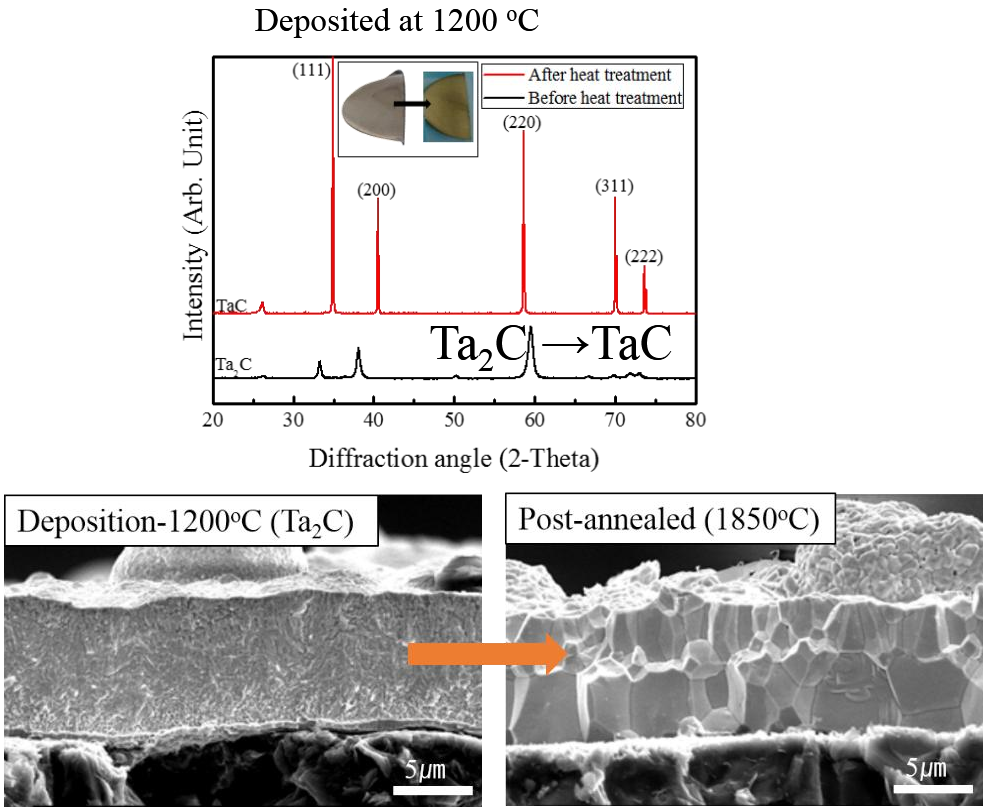

Figure 4. After heat treatment of the specimen with a TaC coating layer deposited at 1200°C, containing Ta_2C phase, XRD and microstructural changes were observed. The XRD analysis revealed a transformation from Ta_2C phase to TaC phase, and the microstructure also changed from columnar to equiaxed morphology.

2. Hafnium carbide deposition on carbon preforms with SiC inter layer

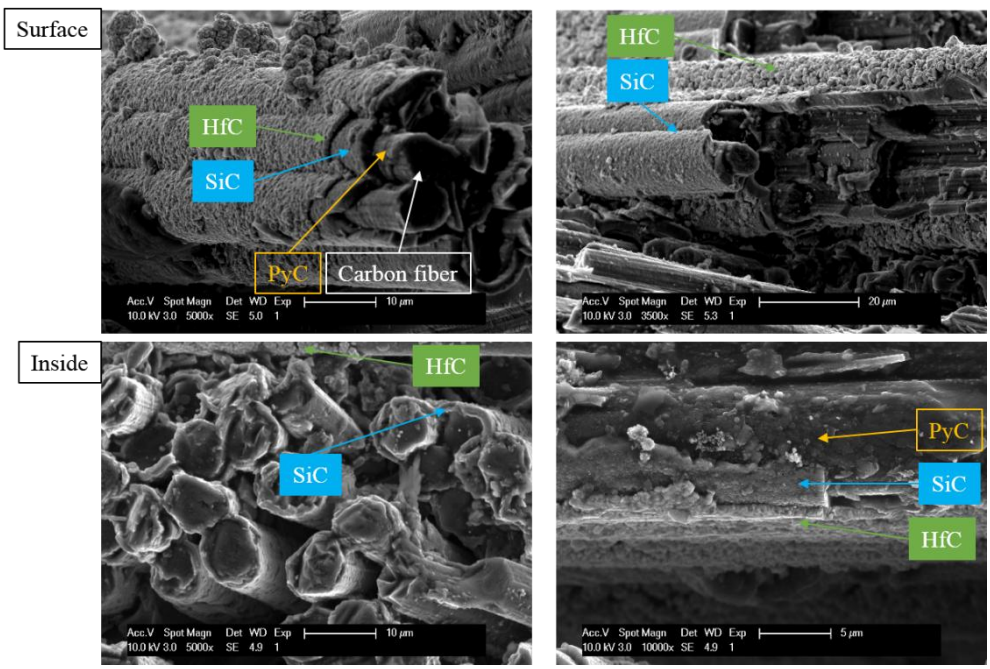

Figure 5. A multi-layer composite was fabricated by sequentially depositing HfC and SiC onto a carbon preform. During this process, it was observed that the HfC coating layer was densely deposited on top of the SiC coating layer.

Table. 1 Deposition condition of HfC-SiC double layer on carbon preform

Phase	Deposition temperature (°C)	Pressure (torr)	Flow rate (sccm)			
			C_3H_6	H_2	$HfCl_4$	CH_3SiCl_3
HfC	1200	50	10	800	91	-
SiC	1000	50	-	74	-	654